COMPARISON OF MACHINE LEARNING MODELS FOR THE POTENTIAL PREDICTION OF TENSILE STRENGTH OF POLY(LACTIC ACID)

by

Seda Serttürk

B.S., in Biomedical Engineering, Biruni University, 2020

Submitted to the Institute of Biomedical Engineering
in partial fulfillment of the requirements
for the degree of
Master of Science
in
Biomedical Engineering

Boğaziçi University
2024

COMPARISON OF MACHINE LEARNING MODELS FOR THE POTENTIAL PREDICTION OF TENSILE STRENGTH OF POLY(LACTIC ACID)

APPROVED BY:

Assoc. Dr. Duygu Ege (Thesis Advisor)	.....
Prof. Dr. Ahmet Ademoğlu (Thesis Co-advisor)	.....
Prof. Dr. Esin Işık	.....
Assist. Prof. Dr. Ceyhun Kırımlı	.....
Assist. Prof. Dr. İpek Şen	.....

DATE OF APPROVAL: 7 June 2024

ACKNOWLEDGMENTS

"Allah'ın lütfuyla"

First and foremost, I would like to extend my infinite thanks to my dear Lord, who is the most gracious and the most merciful.

I would like to express my gratitude to my advisors, Assoc. Prof. Dr. Duygu Ege and Prof. Dr. Ahmet Ademoğlu. Their unwavering support, insightful guidance, and kind encouragement have been invaluable throughout my journey. They provided the motivation and direction needed to overcome challenges and achieve my goals. Their profound insights and critical evaluations have been instrumental in shaping my study, pushing me to think deeply and critically, and build a meaningful project.

My sincere appreciation goes to all the professors and friends in the Institution of Biomedical Engineering (BME). My graduate years were incredibly informative and enjoyable, enriched by collaborative learning experiences. The knowledge and skills I have gained during this time have been truly transformative.

I want to express my deepest gratitude to my dear Mother, dear Father, and dear friends who are like family to me. Your unwavering love and support have been the foundation upon which I have built my all success in my life. I am forever grateful for your presence in my life. Thank you all.

Lastly, I deeply hope for the end of the war in Palestine. May peace come to Palestine and the entire world.

June 7, 2024

ACADEMIC ETHICS AND INTEGRITY STATEMENT

I, Seda Serttürk, hereby certify that I am aware of the Academic Ethics and Integrity Policy issued by the Council of Higher Education (YÖK) and I fully acknowledge all the consequences due to its violation by plagiarism or any other way.

Name :

Signature:

Date:

ABSTRACT

COMPARISON OF MACHINE LEARNING MODELS FOR THE POTENTIAL PREDICTION OF TENSILE STRENGTH OF POLY(LACTIC ACID)

This thesis presents an approach to analyze the 3D printing processes through the application of machine learning (ML) models. We aim to analyse models that predict tensile strength which is a mechanical property of materials, by analyzing the relationship between printing parameters (bed temperature, layer thickness, extrusion temperature, infill density, printing speed) and tensile strength for the printed parts. The primary focus is on determining tensile strength, a critical factor in the functionality and durability of 3D printed objects. Using three different datasets compiled from both published academic research and open-sourced experimental data, we employ four ML regression models -multilinear, support vector, decision tree, and XGBoost- to identify effective predictors of material properties based on printing settings. The thesis's findings highlight the potential for machine learning to significantly increase the precision and efficiency of additive manufacturing. By providing parameters capable of predicting the properties of prints, this approach can save time, reduce material waste, and enable more customized applications of 3D printing in various industries. We also discuss the development of a user-friendly interface to make this tool available to a broader audience, from professionals in the biomedical and aerospace industries to hobbyists and educators. The potential for commercialization through an initial model will also be explored, providing a way to integrate these predictive capabilities directly into 3D printing hardware and software ecosystems. This work advances additive manufacturing and opens new paths for applying machine learning in materials science.

Keywords: 3-Dimensional (3D) Printing, Machine Learning, Tensile Strength, XGBoost, Polylactic Acid (PLA)

ÖZET

POLİ(LAKTİK ASİT)'İN GERİLME MUKAVEMETİNİN POTANSİYEL TAHMİNİ İÇİN MAKİNE ÖĞRENMESİ MODELLERİNİN KARŞILAŞTIRILMASI

Bu proje, makine öğrenimi modellerinin uygulanmasıyla 3B baskı süreçlerini optimize etmek için bir yaklaşım sunmaktadır. Baskılı malzemelerin üretimindeki katman kalınlığı, dolgu yoğunluğu, ekstrüzyon sıcaklığı, baskı hızı, yatak sıcaklığı ve mekanik özellik olan gerilme mukavemeti gibi parametreler arasındaki ilişkiyi analiz ederek, baskı işlemlerinin sonuçlarını tahmin edebilecek modellerin geliştirilmesi ve analiz edilmesi amaçlanmaktadır. Birincil odak, 3B baskılı nesnelerin işlevselliği ve dayanıklılığında kritik bir faktör olan gerilme mukavemetinin belirlenmesidir. Hem yayınlanmış akademik araştırmalardan hem de açık kaynaklı deneysel verilerden derlenen bir veri kümesini kullanarak, baskı parametrelerine dayalı malzeme özelliklerinin etkili tahmin edicilerini belirlemek için karar ağaçları ve XGBoost dahil dört ML regresyon modeli test edilmiştir. Proje bulguları, makine öğreniminin katmanlı üretimin hassasiyetini ve verimliliğini önemli ölçüde artırma potansiyelini vurgulamaktadır. Bu yaklaşım, baskıların özelliklerini tahmin etme becerisi sağlayarak zamandan tasarruf edebilir, malzeme israfını azaltabilir ve çeşitli sektörlerde 3B baskının özelleştirilmiş uygulamalarını mümkün kılabilir. Ayrıca, bu teknolojiyi biyomedikal ve havacılık endüstrilerindeki profesyonellerden hobicilere ve eğitimcilere kadar geniş bir kitleye ulaştırmak için kullanıcı dostu bir arayüzün geliştirilmesi de tartışılmaktadır. Bu yetenekleri, doğrudan 3B baskı ekosistemlerine entegre etmenin bir yolunu sağlayan bir ilk model aracılığıyla ticarileştirme potansiyeli de araştırılmaktadır. Bu çalışma, eklemeli üretimi geliştirmekte ve malzeme biliminde makine öğrenimini uygulamak için yeni yollar açmaktadır.

Anahtar Sözcükler: 3-Boyutlu (3B) Yazıcı, Makine Öğrenmesi, Gerilme Mukavemeti, XGBoost, Polilaktik Asit (PLA)

TABLE OF CONTENTS

ACKNOWLEDGMENTS . . . iii
ACADEMIC ETHICS AND INTEGRITY STATEMENT . . . iv
ABSTRACT . . . v
ÖZET . . . vi
LIST OF FIGURES . . . ix
LIST OF TABLES . . . xi
LIST OF SYMBOLS . . . xii
LIST OF ABBREVIATIONS . . . xiii
1. INTRODUCTION . . . 1
2. BACKGROUND . . . 4
2.1 What is 3-Dimensional (3D) printing? . . . 4
2.1.1 Parameters in 3D Printing . . . 4
2.1.2 Biomedical Use of 3D Printing . . . 7
2.2 Materials . . . 8
2.2.1 Mechanical and Physical Properties of Materials . . . 8
2.2.2 Tensile Strength in Mechanical Properties . . . 9
2.3 What is Polylactic Acid (PLA)? . . . 11
2.3.1 Biomedical Use of PLA in 3D Printing . . . 13
2.4 What is Machine Learning? . . . 14
2.5 Defined Problem . . . 16
2.6 Hypothesis . . . 17
3. METHODOLOGY . . . 18
3.1 Data Collection Process . . . 18
3.2 Computational Modeling . . . 20
3.3 Machine Learning (ML) Models . . . 21
3.3.1 Multiple Linear Regression . . . 22
3.3.2 Support Vector Regression . . . 23
3.3.3 Decision Tree Regression . . . 25
3.3.4 XGBoosting Regression (eXtreme Gradient Boosting Regression) 28

3.4 Validation Methods 30
3.4.1 K-Fold Cross-Validation 30
3.5 Assessing Model Accuracy 31
3.6 Exploratory Data Analysis (EDA) 32
3.6.1 Correlation Heatmap 32
3.6.2 Feature Importance 33
3.6.3 SHapley Additive exPlanations (SHAP) 33
4. RESULTS 34
4.1 Data Summary 34
4.2 Machine Learning (ML) Model Applications 35
4.2.1 Multiple Linear Regression 35
4.2.2 Support Vector Regression 35
4.2.3 Decision Tree Regression 36
4.2.4 eXtreme Gradient Boosting (XGBoost) Regression 37
4.2.5 Evaluation of the Model Performances 39
5. DISCUSSION AND FUTURE WORK 48
5.1 Parameter Effects on the Model Results 50
6. CONCLUSION 54
7. SUPPLEMENTARY DATA 55
REFERENCES 56

LIST OF FIGURES

Figure 2.1 3D-printer schematic diagram: (a) coil reel; (b) filament; (c) motor; (d) extruder; (e) molten paste chamber; (f) nozzle tip; (g) printer bed [1]. It works by utilizing a digital design (a), which is sent to the printer's control system (c). The raw material, likely in the form of filament or resin, is fed through a supply line (b) into the printer's main body. The printer head (e), equipped with a nozzle (f), moves according to the design instructions and lays down the material onto the printing bed (g), layer by layer, to build the 3D object. The material is extruded through the nozzle, which can move both vertically and horizontally within the confines of the printing area, solidifying to form the final object at the printing bed. The platform (g) may also move to assist in the layering process. 5

Figure 2.2 Tensile strength test diagram [2]. It is a mechanical test where a specimen is subjected to a controlled tension until failure. The specimen is held by two grips at both ends, with the upper grip connected to a load cell that measures the force applied to the specimen. The gage length is the part of the specimen that is monitored for elongation. As the crosshead moves downward (indicated by the blue arrow), it stretches the specimen, and the load cell records the force required to do so. This data is used to determine the tensile strength, ductility, and deformation behavior of the material being tested. 10

Figure 2.3 The primary mechanical characteristics derived from a tensile test include: 1. modulus of elasticity; 2. yield strength; 3. tensile strength; 4. ductility; and 5. toughness = 1sdP (measured while under load, which is why the dashed line appears vertical) [2]. 11

Figure 2.4 Polylactic Acid (PLA) chemical structure. [3] 12

Figure 2.5 Machine learning and deep learning differences [4]. 15

Figure 3.1	Machine learning model application workflow.	19
Figure 3.2	SVR plot examples for Linear, RBF and Polynomial kernels with random data.	24
Figure 3.3	Decision tree diagram illustration.	26
Figure 3.4	K-cross validation method illustration [5].	30
Figure 4.1	Correlation heatmap to evaluate the relationship strength between each other for the 1st (a), 2nd (b) and 3rd (c) datasets.	41
Figure 4.2	Illustration of the decision tree for the 3rd dataset, depicting a result of 0.48 obtained in the Decision Tree Regression task.	42
Figure 4.3	Comparison of R^2 results for train and test sets across different machine learning models (MLR, SVR, DTR, XGB) for three datasets. Each boxplot represents a different dataset, showing how each model performs in terms of R^2 scores for both training and testing phases.	43
Figure 4.4	Comparison of Multiple Linear Regression (MLR) model results of three datasets with line of best fits.	43
Figure 4.5	Comparison of Support Vector Regression (SVR) model results of three datasets with line of best fits.	44
Figure 4.6	Comparison of Decision Tree Regression (DTR) model results of three datasets with line of best fits.	44
Figure 4.7	Comparison of XGBoost Regression model results of three datasets with line of best fits.	45
Figure 4.8	Feature importance analysis are illustrated for Decision Tree and XGBoosting regression models.	46
Figure 4.9	SHAP value (impact on model) with beeswarm plot for XGBoost model on the 1st (a), 2nd (b) and 3rd (c) datasets.	47

LIST OF TABLES

Table 3.1	Dataset range for all three of them.	20
Table 3.2	R^2 interpretation.	31
Table 4.1	Summary of the large version of datasets.	34
Table 4.2	SVR linear kernel coefficients representation as weights.	36
Table 4.3	Residuals table for the XGBoost model that used the 3rd dataset.	38
Table 4.4	Machine learning models comparisons by R^2 results for the test set of three versions of datasets.	40
Table 4.5	K-Fold cross validations' R^2 results.	40
Table 7.1	Parameters for 3D Printing and Tensile Strength Values of PLA. All versions of the datasets and model applications scripts are available at: *kaggle.com/sedaserttrk.*	55

LIST OF SYMBOLS

D	Dataset
D_i	Dataset in the ith fold
%	Percentage
°C	Temperature in santigrat degrees
n	Number of observations
m	Size of the subsets
X_n	Predictors
y_i	Actual target values
$\hat{y}_i$	Predicted target values
Y_i	Dependent parameter
$f(x)$	Predicted output
w	Weight vector
k	Subsets
b	Bias term
L	Loss function
M_{-i}	Model that trains on all except ith fold of the data
CV_k	Average error across all k trials
ϵ	Error term
x_i	Independent parameters
α	Hyperparameter
x	Input feature vector
θ_i	Weight
β_0	Intercept
$\beta_n X_n$	Coefficients

LIST OF ABBREVIATIONS

ML	Machine Learning
3D	3-Dimensional
3B	3-Boyutlu
PLA	Poly-lactic Acid
mm	Milimeter
MPa	Megapascal
psi	Per square inch
FDA	Food Drug Administration
XGBoosting	eXtreme Gradient Boosting
AI	Artificial Intelligence
SVR	Support Vector Regression
SVMs	Support Vector Machines
MLR	Multiple Linear Regression
DTR	Decision Tree Regression
MSE	Mean Squared Error
SHAP	SHapley Additive exPlanation
EDA	Exploratory Data Analysis

1. INTRODUCTION

In this thesis, we specifically focus on evaluating the ability of machine learning (ML) models to predict the tensile strength of Polylactic Acid (PLA), a vital property that indicates the material's ability withstanding stress [6]. The analysis is based on examining how the tensile strength of PLA can be affected by various 3D printing parameters, including layer thickness, infill density, extrusion temperature, printing speed, and bed temperature. These parameters are crucial for determining the mechanical properties of 3D-printed objects, and therefore their selection and optimization are essential to achieving the desired performance characteristics in the final product [7],[8],[9].

To analysis the performance of the models, we use a comprehensive approach that leverages various ML regression models to predict tensile strength: Multiple Linear, Support Vector, Decision Tree, and XGBoost. Each of these models offers a unique way to analyze and predict outcomes based on input variables, allowing us to explore a range of analytical techniques in the context of machine learning. Multiple Linear Regression serves as a basic model for understanding linear relationships with multiple parameters, while Support Vector and Decision Tree Regressions provide insights into more complex, nonlinear models [10]. Known for its efficiency and effectiveness in processing various data types and distributions, XGBoosting is used to potentially increase prediction accuracy through advanced boosting techniques [11].

The comparative analysis of these models on the specified parameters aims to determine the most effective approach to predicting PLA tensile strength, taking into account the accuracy, reliability, and applicability of each model. Through this research, we not only evaluate the predictive power of each model but also investigate the effects of parameter selection. This research is intended to contribute valuable information to the integration of machine learning techniques into materials science by providing a path to more complex and informed material selection and design strategies

in the context of additive manufacturing.

In the literature, some research and reviews are highlighting this research topic, with its use areas, effect and importance with different perspectives. Couple of them are mentioned below:

Nasiri and Khosravani (2021) demonstrate the potential of machine learning in improving the prediction accuracy of mechanical behaviors in additively manufactured parts. Their review highlights the critical role of the processing parameters on the performance of the final product and suggests that machine learning can effectively optimize these parameters to optimize the result. It focuses on three domains which are process parameters, porosity prediction which represents the voids or gaps, and defect detection which is for ensuring the quality and reliability of printed parts, have effects on the mechanical behavior of the final 3D-printed parts [12]. This perspective is crucial for developing predictive models that can manage the complexity of 3D printing processes.

Zadpoor (2019) reviews the mechanical performance of additively produced meta-biomaterials, that refers to a biomaterial that is engineered to exhibit unique and enhanced properties which are not found in natural or conventional materials, focusing on their applications as bone substitutes and orthopedic implants. It presents an overview of the effects of the printing processes, material type and bio-functionalization on the mechanical properties (i.e. elastic modulus and yield strength) of additive manufactured meta-biomaterials. The review highlights the importance of establishing accurate topology-property, that also can refer to the mechanical property, relationships, a task well-suited for machine learning models that can address the complex designs and material heterogeneity inherent in meta-biomaterials [13].

Liu et al. (2017) highlight the role of machine learning in materials discovery and design by presenting a framework that can accelerate the development of new materials with optimized properties. Their review shows that ML not only helps in property prediction but also in the discovery of new materials. This is a principle that

can be applied to develop new filaments or resins for 3D printing with special properties [14].

Goh et al. (2020) further expand on the applications of machine learning in various stages of additive manufacturing, from design to process optimization and monitoring. They highlight the transformative potential of machine learning in realizing Industry 4.0 in the 3D printing industry. They also point out significant challenges such as computational costs, data collection techniques, and the need for standardization in data sharing to fully leverage machine learning capabilities [15].

Lastly, Ege et al. (2023), which is our last study, demonstrate a significant advance in tissue engineering by using machine learning to predict how 3D printing parameters affect the tensile strength of Polylactic Acid (PLA) scaffolds. This study highlights the critical role of computational intelligence in improving the scaffold fabrication process, which is crucial for tissue regeneration and engineering. The research marks a leap towards precision and efficiency in biomedical manufacturing by providing a method to systematically optimize scaffold properties by integrating machine learning with additive manufacturing. This synergy promises to accelerate the creation of customized, high-performance biomaterials for regenerative medicine and demonstrates the extensive potential of machine learning in advancing biomedical engineering and materials science through an advanced scaffold production [16].

In this study, we aim to highlight the effect of parameters on tensile strength with ML models and also to analyze the effect of an additional parameter and data set size on the performance of machine learning models using three different data sets, each constrained by certain parameters and number of rows. To perform this analysis, we use four different machine learning models: Multilinear, Support Vector, Decision Tree and XGBoost regression models.

2. BACKGROUND

2.1 What is 3-Dimensional (3D) printing?

The evolution of 3D printing technology, also known as additive manufacturing, has marked a significant milestone in manufacturing and design [17]. 3D printing is a production method by progressively adding material layer by layer following a computer-aided design. It allows for very complex shapes that cannot be made with traditional ways of manufacturing [18]. For example, the aerospace and automotive sectors leverage 3D printing for parts that require specific geometries for efficiency and weight reduction, while the medical field benefits from custom implants and prosthesis tailored to individual patient needs [19],[20]. The use of composite materials and the integration of smart sensors, opening new pathways for innovation in smart manufacturing and beyond [21]. This broad spectrum of applications not only illustrates the adaptability of 3D printing but also its potential to revolutionize traditional manufacturing.

Essential components of a 3D printer include the printing bed, extruder and resin tank, depending on the technology used [22], some of which are illustrated in Figure 2.1. The printers work with a range of materials, from filaments like PLA and ABS to resins and powders, serving diverse applications across industries. The evolution of 3D printing technology aims to enhance speed, precision, material diversity, and accessibility [23].

2.1.1 Parameters in 3D Printing

Parameters in 3D printing are the settings that direct the 3D printer to create an object [24]. These settings include layer height (or thickness), printing speed, extrusion temperature, infill pattern, infill density, and support structures, among others [16],[25].

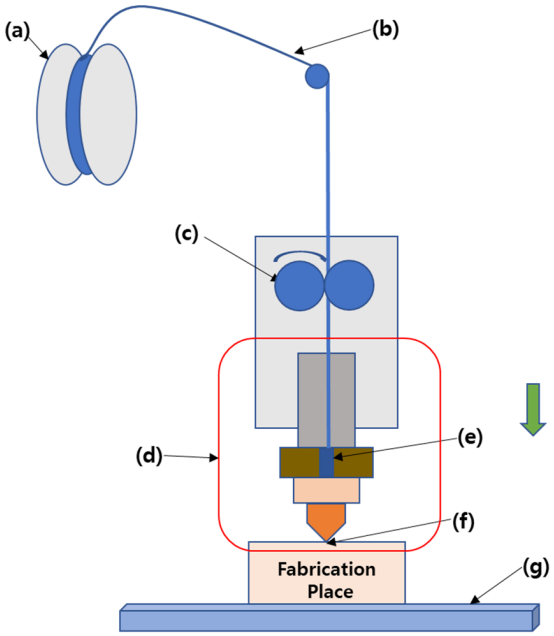

Figure 2.1 3D-printer schematic diagram: (a) coil reel; (b) filament; (c) motor; (d) extruder; (e) molten paste chamber; (f) nozzle tip; (g) printer bed [1]. It works by utilizing a digital design (a), which is sent to the printer's control system (c). The raw material, likely in the form of filament or resin, is fed through a supply line (b) into the printer's main body. The printer head (e), equipped with a nozzle (f), moves according to the design instructions and lays down the material onto the printing bed (g), layer by layer, to build the 3D object. The material is extruded through the nozzle, which can move both vertically and horizontally within the confines of the printing area, solidifying to form the final object at the printing bed. The platform (g) may also move to assist in the layering process.

Parameters are important because they have a direct impact on the quality, appearance, printing time, and mechanical properties of the final product. By adjusting these parameters, users can optimize the 3D printed constructs for specific applications, whether that means achieving finer detail for a prototype, enhancing the strength of a functional part, or reducing material usage and printing time for cost efficiency [26]. Understanding and controlling these parameters allow for the customization of prints to meet exact needs, making them a crucial aspect of the 3D printing process [24].

In this study, five parameters are used: layer thickness, infill density, extrusion temperature, printing speed, and bed temperature. Here, the parameters that are used in the thesis are explained:

1. Layer Thickness (mm): Layer thickness refers to the vertical distance between layers during the printing process and is directly related to the resolution of

the printed object. Setting the layer thickness provides the ability to adjust fine details and smoothness; decreasing the thickness of the layers enhances the precision of the component [8].

2. Infill Density (%): This parameter specifies the amount of material contained within the printed object. Higher infill density (percentages) enhance mechanical properties, although they also lead to increased printing time and material consumption. Infill density is interlinked with infill pattern, layer and wall thickness, and is determined by the specified percentage [27].

3. Extrusion Temperature (°C): The extrusion temperature in 3D printers refers to the temperature at which the material is heated to become molten and flow smoothly through the printer's extruder nozzle. Similar to the presence of a melting point for each material, there exists a specific temperature range that facilitates fluidity. This range not only causes changes in the physical structures of the material, but also has an impact on the mechanical properties of the final product in a 3D printer [28].

4. Printing Speed (mm/s): It refers to the speed at which the extruder moves during the printing process. Adjusting this speed can significantly impact the overall quality of the printed object. Higher speeds can reduce printing time but may lead to lower quality and potential issues. Conversely, slower print speeds generally result in higher quality with more precise details [28].

5. Bed Temperature (°C): In 3D printing, the bed temperature refers to the temperature of the print bed, which is the surface on which the 3D object is printed. The print bed can be heated to various temperatures depending on the material being used for printing. A heated bed helps to prevent the first layers of the extruded material from cooling too quickly, which can lead to warping and other issues that affect the adhesion of the material to the bed and the overall quality of the print [29].

2.1.2 Biomedical Use of 3D Printing

In biomedical engineering, 3D printing technology has revolutionized the production of customized devices and implants by offering precision and customization. This technology has enabled the creation of patient-specific 3D models in cardiology, improved medical teaching, and the development of structural devices [20]. The adaptability of 3D printing is particularly beneficial in complex anatomical areas, where off-the-shelf implants might not offer the best fit or functionality [30].

The pharmaceutical sector also stands to gain from the advancements in 3D printing. It introduces the potential for revolutionizing drug development and manufacturing processes by facilitating the production of medicines with customized dosages and release mechanisms [31]. This advancement aligns with the shift towards personalized medicine, offering tailored treatment options to meet patient needs.

Additionally, the exploration of 4D printing opens new avenues for creating adaptive structures that can respond to environmental stimuli, representing a significant advance in manufacturing capabilities [32]. This convergence of technology and materials science not only expands the scope of 3D and 4D printing, but also improves the functionality and integration of printed objects within biological systems. They have the potential to significantly increase the biocompatibility of printed objects and thus increase their safety and effectiveness for clinical applications [33]. As a result, it paves the way for innovative healthcare solutions and beyond.

As a result, 3D printing has significantly advanced biomedical engineering, enabling precise, customized medical devices and implants. Its expansion into the pharmaceutical industry promises personalized medicine that increase treatment effectiveness. Moreover, the emergence of 4D printing reveals structures that adapt to environmental changes, potentially revolutionizing materials science and clinical applications. Together, these technologies pave the way for innovative and highly personalized healthcare solutions.

2.2 Materials

A material is any substance or matter that can be used to create objects or products. They are typically characterized by their properties, which determine their behavior and suitability for different applications. Materials play a crucial role in manufacturing, construction, and various industries, where they are utilized to produce a wide range of products, from everyday items to advanced and scientific technologies [34]. They are mainly classified into metals, ceramics, and polymers, each with a unique set of properties. For example, metals are characterized by their electrical and thermal conductivity; ceramics are noted for their compressive strength and high melting points; and polymers are known for their low density, high tensile strength, and elasticity. Moreover, composites consist of a combination of two or more distinct types of materials [35].

2.2.1 Mechanical and Physical Properties of Materials

Materials science encompasses the study of the mechanical and physical properties of materials. These properties determine how materials react under various conditions and thus dictate their suitability for specific applications [36]. They include elasticity, tensile strength, hardness, and toughness, whereas physical properties include density, melting point, and thermal and electrical conductivity. Understanding these properties is crucial for selecting materials for engineering applications, designing new materials, and predicting material behavior under different loading and environmental conditions [34],[35],[37].

Mechanical properties define how a material behaves when subjected to mechanical forces or loads, such as stress, strain, and deformation. It is essential for understanding the performance, durability, and suitability of materials for various applications. Some common mechanical properties include elasticity, hardness, toughness, and tensile strength. These properties are typically measured through standardized testing procedures to ensure consistency and accuracy in their assessment [35],[37].

Secondly, physical properties define the characteristics of a material that can be measured or observed without changing the material's chemical composition. They describe the behavior of a material in response to physical stimuli such as temperature, pressure, or electromagnetic fields. Physical properties are inherent to the material and can provide valuable information about its structure, composition, and behavior through density, melting point, boiling point, thermal conductivity, electrical conductivity, and opacity or transparency [35].

Mechanical and physical properties guide the design, selection, and application of materials in various fields, from construction and manufacturing to electronics and aerospace. Advancements in material science continue to push the boundaries of material properties, leading to the development of materials with enhanced performance and novel functionalities [2],[35],[37].

2.2.2 Tensile Strength in Mechanical Properties

Tensile strength (MPa) is a measure of the resistance of a material to break under tension. In other words, it is the maximum amount of tensile stress that a material can withstand before failing or breaking. This property helps to understand how much pulling force or tension a material can bear without deforming or breaking [2].

Tensile strength helps determine whether the printed part is suitable for applications that require strength and resilience, such as in engineering, manufacturing, or product design. Usually, it is expressed in terms of force per unit area, such as newtons per square meter (N/m^2) or pounds per square inch (psi) [35],[37]. It is an essential parameter in materials science and engineering, guiding the choice of materials for different applications based on their intended use and the specific mechanical properties needed [36].

The tensile test, which is illustrated in Figure 2.2, provides a stress-strain curve

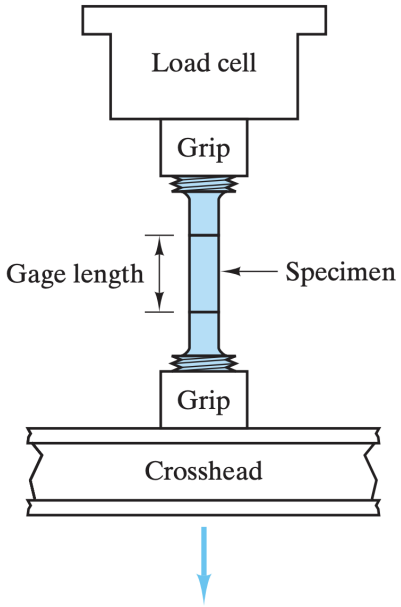

Figure 2.2 Tensile strength test diagram [2]. It is a mechanical test where a specimen is subjected to a controlled tension until failure. The specimen is held by two grips at both ends, with the upper grip connected to a load cell that measures the force applied to the specimen. The gage length is the part of the specimen that is monitored for elongation. As the crosshead moves downward (indicated by the blue arrow), it stretches the specimen, and the load cell records the force required to do so. This data is used to determine the tensile strength, ductility, and deformation behavior of the material being tested.

as in Figure 2.3. Each numbered point on the curve corresponds to a specific mechanical property or behavior of the material under tensile loading: elastic modulus (1), yield strength (2), tensile strength (3), ductility (4), and toughness (5) [2].

The line after the tensile strength indicates that the material is undergoing strain localization, leading to failure. The curve eventually drops down as the cross-sectional area of the material decreases significantly until the material finally breaks [2].

Biomedical Use of Tensile Strength

In biomedical applications, tensile strength is a crucial mechanical property as it determines how a material will resist breaking under tension. This is particularly important for materials that will be subject to forces that try to pull them apart, such as sutures, implants, tissue engineering scaffolds, and wound dressings [2].

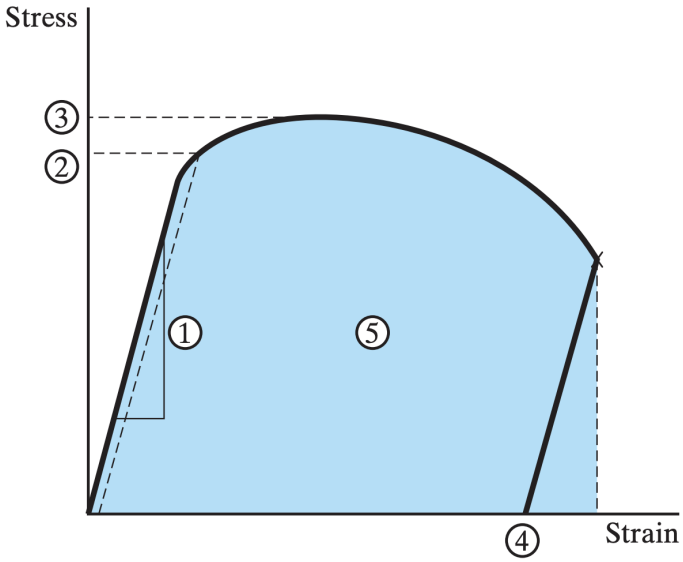

Figure 2.3 The primary mechanical characteristics derived from a tensile test include: 1. modulus of elasticity; 2. yield strength; 3. tensile strength; 4. ductility; and 5. toughness = 1sdP (measured while under load, which is why the dashed line appears vertical) [2].

Materials such as electrochemically deposited conjugated polymer films demonstrate the importance of mechanical properties for the stability of electronic biomedical devices in tissue interfaces, where tensile strength ensures device functionality [38]. In orthopedic applications, Ti-Mn alloys fabricated through powder metallurgy offer a balance between mechanical compatibility with bone tissue and sufficient tensile strength to withstand bodily forces [39]. Additionally, the tensile properties of PLA, which are commonly used in bioresorbable stents and sutures for medical applications, are tailored to enhance mechanical and adhesive properties for tissue treatment applications [40]. These underscore the necessity for strength in materials designed for regenerative medicine. These materials exemplify the diverse role that tensile strength plays in the functionality and success of biomedical devices and materials.

2.3 What is Polylactic Acid (PLA)?

PLA, or polylactic acid, is a biodegradable, bio-based polymer that is synthesized through the ring-opening polymerization of lactide, as depicted in Figure 2.4. It is a type of thermoplastic polyester that originates from renewable sources like sugarcane,

maize, cassava and corn [41].

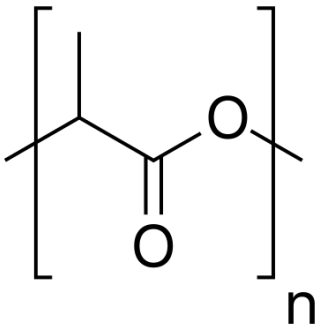

Figure 2.4 Polylactic Acid (PLA) chemical structure. [3]

PLA's physical properties, biocompatibility and biodegradability make it an ideal material for various applications, including packaging, textiles, agricultural and biomedical products [3],[41]. Particularly, it is employed in the production of packaging materials, disposable tableware, and biodegradable medical devices like sutures, screws, and pins used in bone fracture treatments. It mitigates the plastic waste and decrease the environmental impact with its biocompatibility and compostability properties [42]. In recent decades, PLA has gained significant attention, and approval by the U.S. Food and Drug Administration (FDA) for use in biomedical applications due to its low toxicity and good biocompatibility [43].

Additionally, PLA has found utility in the automotive, electronics industries and additive manufacturing (3D printing), where it serves to manufacture lightweight components and casings, thereby enhancing the overall efficiency and sustainability of these products [44].

PLA in 3D Printing

PLA has also demonstrated significant potential in various scientific and technological fields. Recent studies have highlighted PLA's pivotal role, particularly in areas such as energy, agriculture, automotive, and biomaterial sciences, all of which extensively utilize 3D printing technologies [45].

In 3D printing, PLA is used as a filament material, which is melted and extruded layer by layer to create three-dimensional (3D) objects. Its properties, such as a lower risk of warping, ease of processing, and good surface quality, make PLA an excellent material for prototyping, educational purposes, and producing consumer goods. Furthermore, its rheological behavior, low melting temperature, and the fact that it does not emit toxic fumes when heated make it suitable for producing detailed and complex structures in 3D printing technology and its products [46]. PLA-based biomaterials naturally degrade within the body, reduces the need for device removal surgeries and advancing regenerative healthcare [42]. With its array of properties and diverse applications, PLA has become an indispensable material in the field of life sciences.

2.3.1 Biomedical Use of PLA in 3D Printing

The mechanical and physical properties of PLA offer advantages in that they can be easily processed using techniques such as 3D printing, allowing the production of complex structures and customized implants [47]. Additionally, PLA can be modified by incorporating additives or composites to enhance its mechanical properties, addressing issues such as friction, wear, and lubrication of interacting surfaces, thus making it suitable for load-bearing applications [41],[43],[47]. Its versatility allows for biomaterials that are gradually absorbed by the body, minimizing the need for surgical removal and promoting tissue regeneration [42].

PLA is used in 3D printing technologies for medical devices because of its thermoplastic behavior, allowing for the creation of complex structures. Furthermore, PLA can be effectively sterilized using methods like saturated steam, low-temperature steam with formaldehyde, and CO_2 under critical conditions. These sterilization techniques do not cause significant changes in the physicochemical properties of 3D-printed PLA, ensuring its safety and biocompatibility [48]. Furthermore, PLA can be combined with other materials such as ceramic additives, graphene oxide, and calcium phosphate to enhance its biofunctionality and mechanical properties for specific biomedical appli-

cations such as bone tissue engineering [47]. Overall, PLA's unique properties and compatibility with 3D printing make it a suitable material for various biomedical applications.

2.4 What is Machine Learning?

The field of machine learning (ML), a foundationstone of artificial intelligence (AI), has its roots in the early days of computer science and cognitive psychology. In the 1950s, the concept of machines learning from data and improving over time was first considered, with pioneers such as Alan Turing proposing the idea of a "learning machine" that could simulate human intelligence [49]. This period marked the beginning of exploring algorithms that could enable computers to perform tasks without being explicitly programmed for each specific task.

In the following decades, significant theoretical developments and foundational algorithms were produced. In the 1960s and 1970s, researchers developed the perceptron, an early neural network model, and decision trees, setting the stage for the development of more complex models [50]. During the 1980s and 1990s, significant advancements were made with the introduction of crucial concepts like the backpropagation algorithm, enabling the training of multi-layer neural networks, and support vector machines, which provided a strong framework for classification and regression tasks [51],[52].

Machine learning stands at the intersection of computer science and statistics, with progress in artificial intelligence and data science. The rapid growth of it is driven by the online data and affordability of computation, which has led to its widespread adoption across various domains, including healthcare, manufacturing, education, and more, facilitating evidence-based decision-making (Figure 2.5) [53].

When we look at the technical background of ML, the basic principle is that computers gain understanding from data, identify patterns, and make decisions with

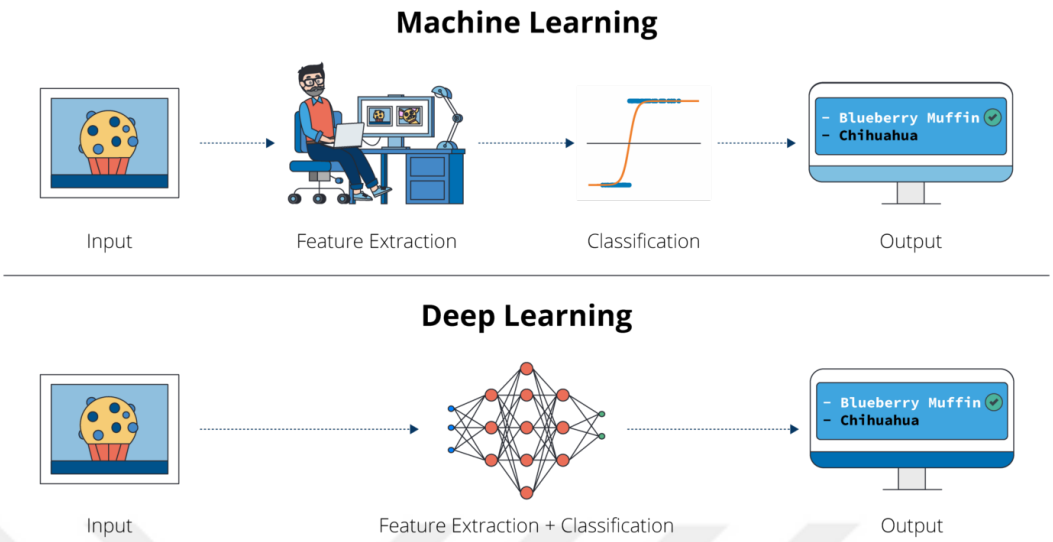

Figure 2.5 Machine learning and deep learning differences [4].

minimal human guidance. It begins with collecting relevant data that is critical and can include various data types such as text, images, and numerical values. This data is then prepared and cleaned, a process that may include handling missing values, normalizing data scales, and dividing the data into subsets for training and testing. The choice of ML model is necessary and depends on the problem type (classification, regression, or clustering) and data characteristics [54].

The training step involves tuning the model based on its performance, where the model learns from its errors under supervision for tasks with previously known outcomes or attempts to directly identify patterns in unsupervised tasks without knowing. After training, the model's ability to generalize and perform on unseen data is evaluated using the test set. Depending on the outcome of this evaluation, the model may undergo further tuning to improve its parameters and improve prediction accuracy or decision-making ability. Once a model demonstrates satisfactory performance, it can be used in real-world applications where it continues to learn from new data, thus improving its accuracy and adaptability over time [55].

The application of ML in biology and medicine demonstrates its transformative

potential, from increasing diagnostic accuracy to providing personalized treatments. ML algorithms improve the understanding of complex biological processes and disease mechanisms by facilitating the analysis of genetic and genomic data [56]. Additionally, the exploration of biological networks through ML opens up possibilities for novel therapeutic strategies and drug discovery [31].

Machine learning is rapidly transforming many fields, enhancing our understanding of complex systems, and driving innovations. As it integrates further across different scientific areas, machine learning promises to unlock new discoveries and improve the world through data-driven insights. This technology exemplifies the advancements possible when we effectively utilize the power of data [57].

2.5 Defined Problem

In biomaterial studies, the advancement of technological approaches in material science has enabled researchers to utilize 3D printing for fabricating complex biomaterial products for various applications [33]. In both material and biomaterial sciences, understanding the mechanical and physical properties is essential to determining how materials behave under different conditions [37]. Currently, figuring out the best parameter settings for creating materials is mostly done by scientific methods such as Taguchi and Design of Experiments (DOE), which systematically explore the effects of multiple variables on performance outcomes. Engineers often create several versions, test them, and iterate until the optimal settings are found.

Now, machine learning is changing the game by quickly sorting through data to find optimized printing settings. This smart approach cuts down on wasted time and materials, helping to push the field forward to make new and optimized products. However, precisely predicting the mechanical and physical properties of these materials remains a considerable challenge [58]. Even with these advances, we still need to check the final products to make sure they meet high standards and work the way they should.

2.6 Hypothesis

Our hypothesis employs machine learning methodologies to investigate the impact of five parameters (layer thickness, infill density, extrusion temperature, printing speed, and bed temperature) on the tensile strength of Polylactic Acid (PLA) material [58]. We compiled a comprehensive dataset by collecting experimental data on PLA across various combinations of these parameters. Using regression-based machine learning models, we will analyze the complex relationships between these input parameters and the tensile strength of PLA. These models will undergo evaluation using cross-validation techniques and hyperparameter tuning to optimize performance measurements. The findings will be illustrated through visualizations, including feature importance and SHAP analysis graphs, providing insights into the relative importance of each parameter in determining the tensile strength of PLA.

3. METHODOLOGY

In this thesis, our focus has been on supervised learning models to predict tensile strength as y_i based on the inputs as x_i, following a common example of a linear model. In this model, the prediction is given by $\hat{y}_i = \sum_j \theta_i x_{ij}$, where $\hat{y}_i$ is the predicted tensile strength for the i-th sample. The equation represents a linear combination of weighted input features, with θ_i serving as the weight or coefficient corresponding to each feature x_{ij}, indicating the strength of influence each parameter has on the outcome. This approach assumes a linear relationship between the dependent variable and the independent variables, which is typical in regression analysis, allowing us to quantify how different parameters contribute to the tensile strength of the materials studied. Here, four supervised models are utilized to compare their efficiency for our datasets: multiple linear (multilinear), support vector, decision tree, and extreme gradient boosting (XGBoosting), which is a gradient-boosted decision tree regression model. These models are compared based on their R^2 results.

In the thesis, we follow the flow in Figure 3.1 and divide the data into 20% and 80% for test and training sets, respectively. Using the training set, the prediction models are built and adjusted with hyper-parameters for XGBoosting. To scale the data, normalization is applied. Further details about hyper-parameter adjustments applied in the model can be found in Section 4.2.4, which provides detailed information.

3.1 Data Collection Process

The data collection process considered a range of variables, parameters, and material types. More than 50 articles focusing on the 3D-printed PLA material, along with several open-access datasets, are reviewed. Out of these, three different articles, Jattie et al. (2022) [58], Hikmat et al. (2021) [59], Gao et al. (2022) [60] and one open-access dataset [61], are utilized for this thesis. Our study compares machine learning model performances on different datasets to evaluate the impact of five parameters

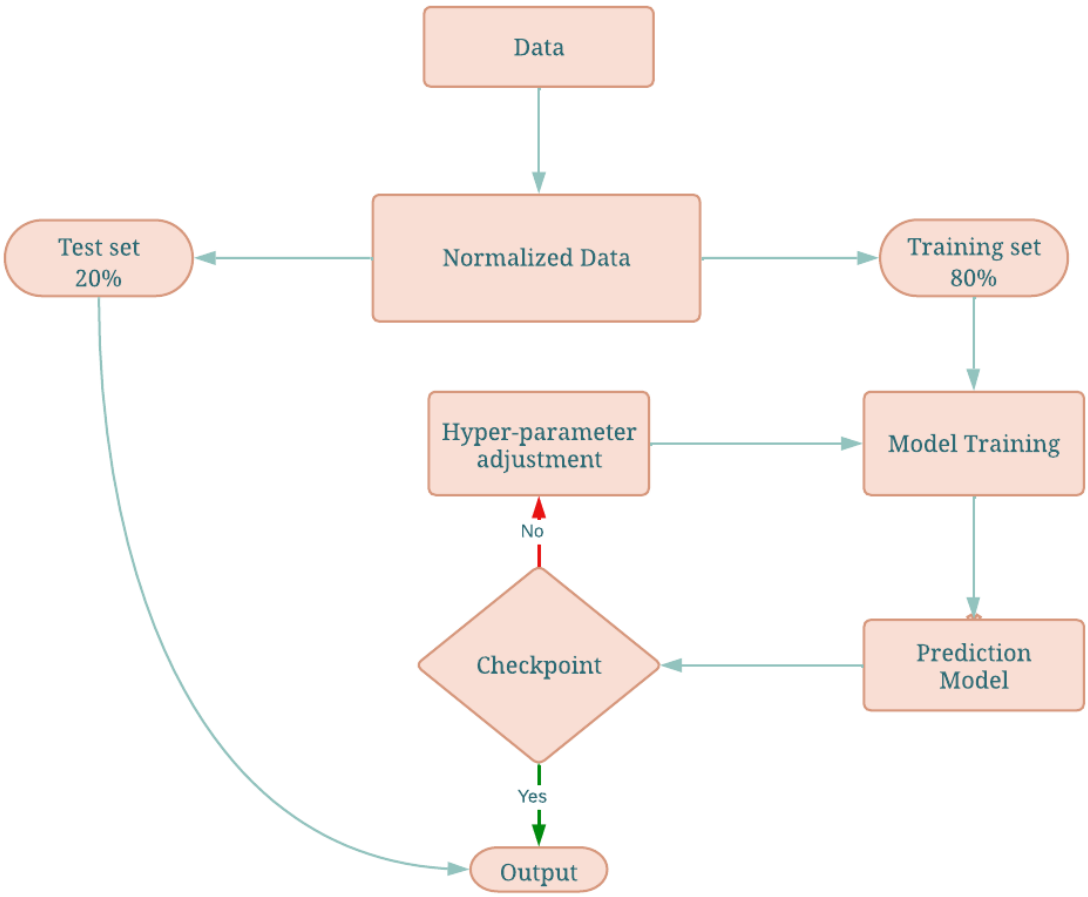

Figure 3.1 Machine learning model application workflow.

on the tensile strength of Polylactic Acid (PLA). Using regression-based models and comprehensive experimental data, we analyze these relationships, employing cross-validation and hyperparameter tuning. Visualizations, including feature importance graphs, will identify key factors, helping to optimize production processes by reducing variation and ensuring robustness.

As shown in the research of Popescu et al. (2018) [62] and in other studies that mentioned respectively, several parameters affect the mechanical properties of the final product in 3D printing: layer thickness [63], infill density [64], air gap, raster orientation [65], temperature [66], feed rate, build orientation and printing speed [67]. Surely not all parameters exert an equal influence on determining the characteristics; in light of the scarcity of reliable data, the number of parameters are constrained to

Table 3.1
Dataset range for all three of them.

#	Row	Parameters
1	58	layer thickness, infill density, extrusion temperature, printing speed
2	58	layer thickness, infill density, extrusion temperature, printing speed, bed temperature
3	107	layer thickness, infill density, extrusion temperature, printing speed

five factors: layer thickness, infill density, extrusion temperature, printing speed, and bed temperature. In this study, three different datasets are created to compare both the effect of the bed temperature as fifth parameter and size of the datasets; with four different machine learning models (Table 3.1).

3.2 Computational Modeling

All machine learning models implemented with Python programming language with NumPy, Pandas, Scikit-learn, Matplotlib, Seaborn and XGBoost libraries, since Python is a very common programming language and also it has easy-to-understand and an applicable format, gives better results and implentable.

- NumPy is essential for scientific computing with Python, offering a library that supports multidimensional arrays, various objects like masked arrays and matrices, and numerous functions for rapid array operations. These functions encompass mathematical and logical operations, array reshaping, sorting, alongside capabilities in discrete Fourier transforms, linear algebra, statistics, and random number generation [68].

- Pandas is an open-source tool for data analysis and manipulation that's both efficient and user-friendly, developed for the Python programming language. It offers robust and fast capabilities for handling complex data operations [69].

- Scikit-learn is a machine learning library for Python, offering tools for both supervised and unsupervised learning. It includes functionalities for fitting models,

preprocessing data, selecting models, evaluating them, and other various utilities [70].

- Matplotlib is a versatile library in Python for generating static, animated, and interactive visualizations. It simplifies the creation of high-quality plots and interactive figures that offer zooming and panning capabilities. Users can customize the visual appearance and layout, export visualizations in various formats [71].

- Seaborn is a library for data visualization in Python, built on matplotlib. It offers an advanced interface for creating visually appealing and informative statistical charts [72].

3.3 Machine Learning (ML) Models

In machine learning (ML), understanding basic terms such as loss, objective, and cost functions is essential to understanding how algorithms learn and make decisions. The loss function, also known as the cost function, measures how far off the model's predictions are from the actual values in the dataset. It helps guide the model during training by indicating the errors that need to be minimized [73]. The objective function, closely related, often encompasses the loss function and possibly regularization terms; its minimization (or maximization, depending on the context) is the goal of the learning algorithm [5],[74]. Understanding these concepts is foundational for delving deeper into the mechanics of machine learning models and their optimization processes. Normalization, another important concept, involves adjusting the values measured on different scales to a common scale, typically within the range of 0 to 1 or -1 to 1. This process ensures that no single feature dominates the learning process due to its scale, facilitating better model performance and faster convergence [75].

Normalization is a crucial preprocessing step in machine learning, commonly implemented using the min-max scaling technique. This method is defined as follows [75]:

$$X_{normalized} = \frac{X - X_{min}}{X_{max} - X_{min}} \tag{3.1}$$

where X is a feature value to be normalized, X_{min} is the minimum value of the feature in the dataset, and X_{max} is the maximum value of the feature in the dataset. This normalization technique ensures that the features are scaled within a specific range, facilitating better model performance and faster convergence.

3.3.1 Multiple Linear Regression

Multiple Linear Regression (MLR) is a branch of linear regression models that stands as a foundational statistical technique within the machine learning, serving as a flexible model for understanding and quantifying relationships between multiple predictors and a singular outcome variable [76].

The formal representation of MLR is [76]:

$$Y_i = \beta_0 + \beta_1 X_1 + \beta_2 X_2 + \ldots + \beta_n X_n + \varepsilon_i \tag{3.2}$$

Here in:

- Y_i represents the dependent variable, indicative of the outcome subjected to predictive analysis in ith trial.
- β_0 defines the intercept, encapsulating the expected value of Y_i when all predictor variables $X_1, X_2, \ldots, X_n$ are maintained at zero.
- $\beta_1, \beta_2, \ldots, \beta_n$ define the coefficients corresponding to the respective predictor vari-

ables, explaining the change in Y_i per unit adjustment in the associated X, while holding other predictors constant.

- $X_1, X_2, \ldots, X_n$ defines the predictor variables, collectively influencing the predictive outcome.
- ε_i is the error term, embodying non-observable factors affecting Y_i that remain unaccounted for in the model.

In the machine learning context, Multiple Linear Regression (MLR) holds significant importance for modeling relationships within datasets. Its versatile application extends across various fields, such as healthcare, social sciences, finance, and economics, where predictive analytics and understanding the interplay between multiple variables [77]. The operationalization of MLR involves key steps, including the estimation of coefficients through statistical methods, subsequent validation of the model, and a comprehensive assessment of its predictive impact [76],[78].

3.3.2 Support Vector Regression

Support Vector Machines (SVMs) are typically employed for classification problems; however, they can also be utilized for regression tasks, referred to as Support Vector Regression (SVR). In regression scenarios, SVR is designed to predict a continuous output variable instead of discrete class labels. The fundamental principle underlying SVR involves constructing an epsilon-insensitive tube around the hyperplane, introducing a specified level of tolerance (ϵ) for prediction errors [5],[78].

SVR aims to achieve a balance by minimizing prediction errors while allowing for flexibility within the epsilon-insensitive tube, where it defines the width of the tube within which no penalty is associated with predictions that deviate from the actual values [5],[74]. A hyperplane, in the context of support vector, is a decision boundary that separates different surfaces in the feature space. It can efficiently manage both linear and non-linear relationships within the data, offering a dependable solution for

regression tasks that require capturing complex patterns to enhance prediction accuracy [5]. These concepts are illustrated with random data for each kernel in Figure 3.2.

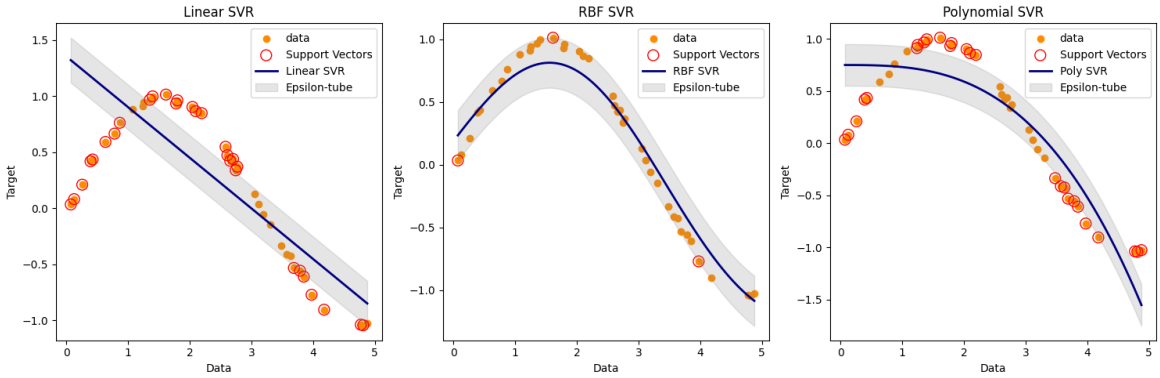

Figure 3.2 SVR plot examples for Linear, RBF and Polynomial kernels with random data.

In linear SVR, the algorithm aims to find a linear hyperplane that best fits the data within the epsilon-insensitive tube. This hyperplane is determined by optimizing coefficients while considering the tolerance level (ϵ) for errors. Linear SVR is effective when the relationship between input features and the target variable is approximately linear, and it utilizes the epsilon-insensitive tube to account for variations in the data while maintaining the linearity of the model [55].

The SVR model with a linear function is represented as [79]:

$$f(x) = \langle w, x \rangle + b \tag{3.3}$$

- $f(x)$ is the predicted output.
- $\langle w, x \rangle$ is the dot product of the weight vector w and the input feature vector x.
- b is the bias term.

In nonlinear SVR, the algorithm goes beyond the constraints of linear relation-

ships and allows for the modeling of more complex, nonlinear patterns in the data. Rather than using a linear hyperplane, nonlinear Support Vector Regression (SVR) employs a kernel trick to project the input features into a higher-dimensional space. This approach allows the algorithm to identify a hyperplane that more accurately reflects the relationships in the data [78].

The selection of a kernel function in Support Vector Regression (SVR) is crucial for modeling nonlinearity. The Radial Basis Function (RBF) kernel, often used in SVR, calculates the similarity between data points radially, making it suitable for capturing complex, nonlinear relationships. Alternatively, the polynomial kernel enables the model to fit a polynomial regression curve that adapts to data curvature. These kernels assist in transforming the original feature space into a higher-dimensional space, facilitating the discovery of a linear separator. SVR also uses an epsilon-insensitive tube, which establishes a threshold within which errors are ignored, allowing the model to ignore minor deviations and focus on more significant trends. This feature is particularly beneficial for handling data variability in the transformed space [5],[78].

3.3.3 Decision Tree Regression

A decision tree is a supervised learning algorithm employed for tasks involving both classification and regression and serves as a basic component of Random Forests [78]. Its hierarchical tree structure includes a root node, branches, internal nodes, and leaf nodes. Decision trees facilitate the interpretation of decisions, the identification of potential events, and the visualization of likely outcomes. This analysis contributes to determining the optimal decision [80],[81].

As shown in Figure 3.3, a decision tree starts at a root node, which has no incoming connections. The branches emanating from this root node extend to internal nodes, also referred to as decision nodes. Both root and internal nodes evaluate available features to group similar instances, forming leaf nodes or terminal nodes. Each branch in the tree corresponds to a specific condition based on the factors, with

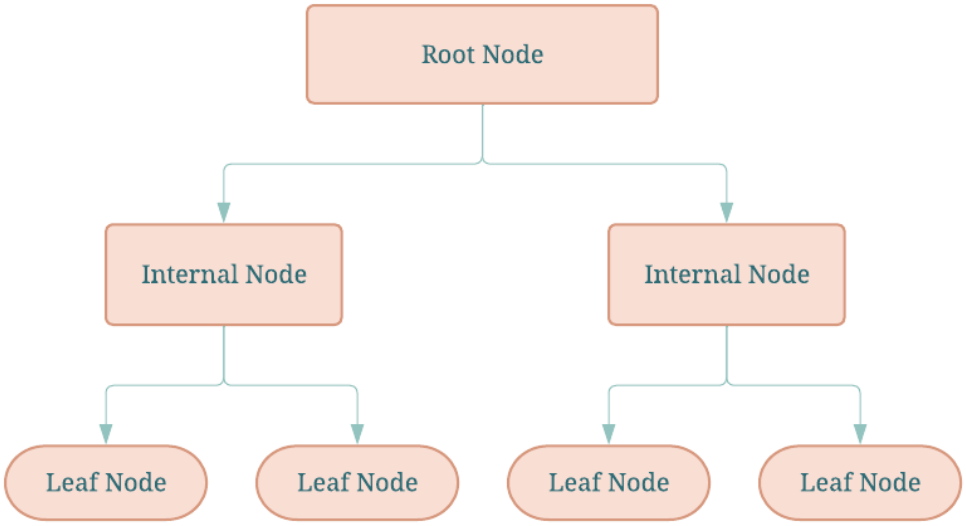

Figure 3.3 Decision tree diagram illustration.

associated threshold values guiding the decision-making process. The terminal points of the branches, referred to as "leaf nodes", provide the model's predictions for the target variable. These predicted values represent the model's estimate of the average or median of the target property under those specific conditions. The leaf nodes in a decision tree depict all the potential outcomes within the dataset [80].

Decision tree structures, with their easily comprehensible flowchart format, facilitate a clear representation of decision-making processes, enabling various organizational groups to understand the rationale behind decisions. In decision tree learning, iteratively identifying optimal split points within the tree to classify records under specific class labels. The quest for pure leaf nodes, representing homogenous sets, is influenced by the tree's complexity, with smaller trees achieving purity more easily. However, larger trees may face challenges, leading to data fragmentation and potential overfitting. To address this, pruning is applied to remove branches with low-importance features, promoting simplicity and adherence to the principle of Occam's Razor which promotes a simpler solution by eliminating unnecessary components, thereby improving the model's effectiveness and making it easier to understand [78]. Cross-validation evaluates the model's fit, and to enhance accuracy, decision trees can be aggregated into an ensemble, such as a random forest algorithm, particularly effective when individual

trees exhibit low correlation [81].

Information gain, calculated as the reduction in entropy after a split, guides the algorithm in selecting the best features for decision points. For regression tasks, decision trees use measures like mean squared error (MSE) to assess the variance of target values. The training process involves recursively optimizing splits to minimize impurity measures. Pruning, a technique that removes branches contributing little predictive power, helps prevent overfitting. Decision trees follow a greedy algorithm, making locally optimal decisions at each step, leading to a versatile and interpretable model for various machine learning tasks [81].

1. **Prediction in Leaf Nodes**

   In decision tree regression, each leaf node corresponds to a particular area in the feature space. The predicted value for that area is derived from the average (or weighted average) of the target variable for the training instances that fall into that area.

2. **Objective Function - Mean Squared Error (MSE)**

   Decision tree regression works to reduce the Mean Squared Error (MSE) in all its leaf nodes. MSE is the average of the squared differences between the actual target values (y_i) and the predicted values ($\hat{y}_i$):

$$MSE = \frac{1}{n}\sum_{i=1}^{n}(y_i - \hat{y}_i)^2 \tag{3.4}$$

   where n is the number of data points, y_i is the actual target value, and $\hat{y}_i$ is the predicted target value.

3. **Recursive Splitting and Splitting Criteria**

   The decision tree algorithm employs a recursive, top-down approach to select the best feature and split point. The best feature is the variable that, when used for splitting the data, minimizes the Mean Squared Error (MSE) of the

resulting subsets, effectively enhancing the model's accuracy and efficiency. At each internal node in a decision tree, a specific feature and threshold are selected to split the data into smaller subsets.

$$WeightedMSE = \frac{m}{n} \times MSE_{left} + \frac{n-m}{n} \times MSE_{right} \tag{3.5}$$

where m and $n - m$ are the sizes of the left and right subsets, and MSE_{left} and MSE_{right} are the MSE for each subset.

4. **Tree Pruning**

   Since decision trees can become complex and prone to overfitting, pruning involves removing branches to improve generalization. Cost-complexity pruning introduces a hyperparameter (α) to penalize complex trees:

$$Cost - complexity = MSE + \alpha \times Complexity \tag{3.6}$$

   The complexity term is a measure of the number of terminal nodes.

5. **Training and Prediction**

   The decision tree is trained by recursively selecting features and split points to minimize the MSE, and to predict the target value for new data, the algorithm transverses the tree based on the feature values until it reaches a leaf node. The predicted value is determined by the average (or weighted average) of target values in that leaf [5],[78],[80],[81].

3.3.4 XGBoosting Regression (eXtreme Gradient Boosting Regression)

XGBoost stands for "eXtreme Gradient Boosting" with the term "Gradient Boosting" originating from Friedman's paper titled "Greedy Function Approximation: A Gradient Boosting Machine" [82].

Gradient boosting constructs a predictive model by combining multiple simple models, typically decision trees, one after another. Each model is trained to correct the mistakes of the ensemble thus far. This process uses a method similar to gradient descent to optimize a particular loss function, ensuring every new tree concentrates on the errors from the previous trees. As a result, the model becomes more accurate with each step. In regression tasks, the objective of gradient boosting is to reduce the residuals, which are the differences between the actual values and the ensemble's predictions [11]. This technique effectively uncovers complex patterns in the data, leading to increasingly accurate predictions [5],[83].

XGBoost is an advanced implementation of gradient boosting that includes regularization to prevent overfitting, parallel processing to speed up computations, and strategies to manage missing data. While it maintains the step-by-step model training characteristic of gradient boosting, XGBoost adds enhancements that boost its efficiency, precision, and effectiveness in diverse scenarios. These improvements have made XGBoost a popular choice in machine learning competitions and practical applications [83],[84],[85].

Application of the Model

In summary, the XGBoost regression model's application begins by defining an objective function to minimize, often involving a mean squared error (MSE) for regression tasks. The model iteratively builds a series of decision trees, where each successive tree rectifies the errors made by its predecessors. These trees are intentionally shallow to help prevent overfitting and enable faster training. During each iteration, XGBoost assigns weights to data points based on their previous residuals, placing more emphasis on the points that the model struggled to predict accurately [82],[83],[84].

Throughout the thesis, while the residuals may not be directly observable at each step, the model calculates them continuously in the background as part of its internal processing. Furthermore, XGBoost applies regularization techniques to manage the

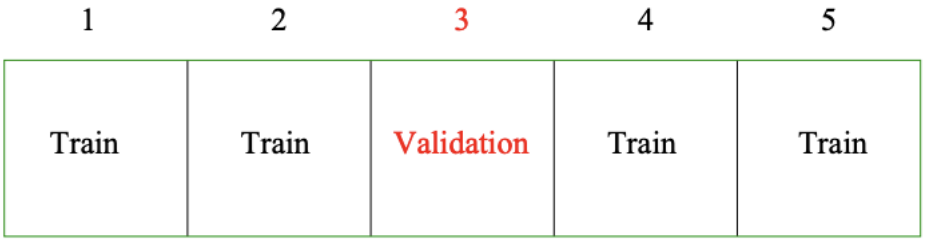

Figure 3.4 K-cross validation method illustration [5].

complexity of the trees it constructs. The model aggregates the predictions from all trees to deliver the final regression outcome after a specified number of iterations or upon meeting a predetermined stopping criterion [11],[84].

3.4 Validation Methods

Validation methods are essential in machine learning for ensuring a model's ability to generalize to new, unseen data by evaluating its performance during training. K-Fold Cross-Validation is frequently employed, dividing the dataset into k separate folds to maximize data utilization and estimate performance effectively. The method provides valuable insights into a model's expected performance on unseen data [5],[86].

3.4.1 K-Fold Cross-Validation

K-Fold Cross-Validation is a method for evaluating how well machine learning models perform. Here's how it works: the dataset is divided into k equal parts, or "folds." The model is then trained on $k-1$ of these folds, while the remaining fold is used as a test set. This process is repeated k times, with each of the k folds used as the test set once. After all rounds are completed, the average performance across all k tests is calculated. This approach helps to reliably assess the model's effectiveness [5].

Mathematical Background

When D is a dataset containing n observations. The dataset is randomly divided into k folds, $D_1, D_2, \ldots, D_k$, each of approximately equal size. The training and validation process is as follows:

$$CV_k = \frac{1}{k} \sum_{i=1}^{k} L(D_i, M_{-i}) \tag{3.7}$$

where L is the loss function, D_i represents the data in the ith fold and M_{-i} represents the model that trains on all but ith fold of the data. The goal is to minimize CV_k, the average error across all k trials [5].

3.5 Assessing Model Accuracy

Mean Squared Error (MSE) and the coefficient of determination (R^2) are crucial metrics used to evaluate regression models. A higher R^2 value indicates that the model has a greater degree of accuracy in predicting outcomes [5].

Table 3.2
R^2 interpretation.

R^2 Values	Interpretation
< 0.6	Unsatisfactory prediction
0.6 - 0.75	Satisfactory prediction
> 0.75	Excellent prediction

MSE, yielding:

$$MSE = \frac{1}{n}\sum_{i=1}^{n}(y_i - \hat{y}_i)^2 \tag{3.8}$$

R^2, on the other hand, offers understanding of the proportion of variance in the dependent variable that can be explained by the independent variables, as expressed by:

$$R^2 = 1 - \frac{\sum_{i=1}^{n}(y_i - \hat{y}_i)^2}{\sum_{i=1}^{n}(y_i - \bar{y})^2} \tag{3.9}$$

where $\bar{y}$ is the mean of observed values. An R^2 value of 1 indicates perfect explanatory power, whereas a value of 0 indicates none for it [5].

3.6 Exploratory Data Analysis (EDA)

Exploratory Data Analysis (EDA) is a statistical technique that helps to understand data sets better by summarizing their main characteristics, often through visualization. EDA is mainly used to explore what the data reveals before engaging in more formal modeling or hypothesis testing, allowing for a more casual approach to analyzing data. In this study, we employ various methods including correlation heatmaps, assessments of feature importance, and SHapley Additive exPlanations (SHAP) to derive important insights from the data.

3.6.1 Correlation Heatmap

A correlation heatmap is a visual representation of the data in a correlation matrix, providing a visual summary of how the variables in a dataset are related to

one another. The heatmap displays the degree of correlation between pairs of variables using color codes. Areas of high positive correlation may be represented by one color, high negative correlation by another, with neutral correlation by a third color, these allow quick identification of relationships and patterns [87].

3.6.2 Feature Importance

Feature importance in machine learning is a technique used to identify which features in your dataset have the most influence on the outcomes of the models. It quantifies the contribution each feature makes to the model's predictions, allowing you to understand which variables are most predictive and should be focused on for model training and interpretation. Specifically, feature importance works by quantifying the impact of each input variable on the predictive accuracy of a model. This is achieved by measuring how the prediction error increases when the data for that feature is altered or randomized. This method guides more informed decisions about the selection and prioritization of features in model development, ensuring that resources are allocated effectively and that the model is both efficient and powerful in making predictions [88].

3.6.3 SHapley Additive exPlanations (SHAP)

SHAP (SHapley Additive exPlanations) is a technique that uses principles from game theory to interpret the output of any machine learning model. It employs Shapley values to allocate credit for a prediction optimally, considering both the importance of each feature and how features interact to influence the model's output [89].

In a scatter plot for SHAP analysis, i.e., Figure 4.9, data points to the left of the zero line indicate a negative impact. The color of points corresponds to the feature value: low values are in pink/blue, and high values are in red/dark blue in this thesis [90].

4. RESULTS

4.1 Data Summary

Here, we have three different datasets, each representing a different concept. The first dataset, our base dataset, has 4 parameters (layer thickness, infill density, extrusion temperature, and printing speed) and contains 58. The second dataset includes these 4 parameters plus bed temperature, containing 58. The third dataset is a larger version of the first dataset, containing 107. The inclusion of smaller and larger versions of the first dataset allows us to analyze the impact of dataset size on R^2 results. We aim to analyze the effect of bed temperature with the second dataset and compare the R^2 results between the small and larger datasets, as seen in Table 3.1 (For a summary of the large version of the dataset: Table 4.1).

Table 4.1
Summary of the large version of datasets.

	Layer Thickness (mm)	Infill Density (%)	Extrusion Temperature (°C)	Printing Speed (mm/s)	Bed Temperature (°C)	Tensile Strength (MPa)
Mean	0.19	70.68	212.29	52.38	69.75	37.27
Median	0.18	78	210	50	70	36.17
Mode	0.15	100	210	60	70	12
STD	0.1	28.62	8.16	20.65	5.33	12.79
Min	0.02	10	190	20	60	4
Max	0.4	100.5	120	120	80	60.29
#	107	107	107	107	58	107

The datasets are visualized in Figure 4.1 to see the correlations between tensile strength, layer thickness, infill density, extrusion temperature, printing speed, and bed temperature for each dataset utilizing the heatmap. Maximum correlations for tensile strength are observed in infill density for the 1st and 2nd datasets and in layer thickness for the 3rd dataset.

4.2 Machine Learning (ML) Model Applications

In this thesis, four regression models are applied: Multiple Linear Regression (MLR), Support Vector Regression (SVR), Decision Tree Regression and XGBoost to analyze the relationship between tensile strength and the independent input parameters.

4.2.1 Multiple Linear Regression

The Multiple Linear Regression (MLR) model is used to predict the tensile strength of PLA across three datasets. In Figure 4.4, the graph compares the actual and predicted tensile strength of the model. The model performs well on the 1st and 2nd datasets, with R^2 scores of 0.69 and 0.73, respectively. However, it performs poorly on the 3rd dataset, with an R^2 of 0.37, suggesting issues with data complexity or quality.

MLR models for the 1st and 2nd datasets show close R^2 scores between the training and test sets, indicating better generalization and less overfitting. The 1st dataset has R^2 scores of 0.77 (Train) and 0.69 (Test), while the 2nd dataset shows 0.78 (Train) and 0.73 (Test), as seen in Figure 4.3. Conversely, the MLR model on the 3rd dataset shows lower R^2 scores across all sets, with 0.34 (Train) and 0.37 (Test), suggesting weaker performance and potential underfitting. These results highlight the reliability and generalization capability of MLR models on the 1st and 2nd datasets, while the 3rd dataset may require further refinement to enhance its performance.

4.2.2 Support Vector Regression

Support Vector Regression (SVR) was utilized with linear kernel. The linear kernel yielded R^2 values of 0.69, 0.71, and 0.11 for the datasets (Figure 4.5). Applying the linear kernel reveals the coefficients and bias, which represent the hyperplane (Table

4.2). These details are not shown in Figure 4.5, which only illustrates the linear function itself.

As shown in Figure 4.3, the SVR models demonstrate varying performance across the datasets. For Dataset 1, the model shows performance with R^2 scores of 0.50 (Train) and 0.69 (Test), indicating better performance in the test set. Dataset 2 performs exceptionally well with R^2 scores of 0.50 (Train) and 0.71 (Test), showing strong predictive capability. In contrast, Dataset 3 exhibits very low R^2 scores, especially on the training set (0.09), suggesting significant underfitting. These results highlight the importance of model selection and tuning for different datasets to achieve optimal predictive performance.

Table 4.2
SVR linear kernel coefficients representation as weights.

	Dataset 1	Dataset 2	Dataset 3
Layer Thickness	5.57575758	5.57575758	6.44736842
Infill Density	7.2	7.2	1.25966851
Extrusion Temperature	0.66666667	0.66666667	−0.875
Printing Speed	−2.6875	−2.6875	−1.7
Bed Temperature	–	1.0	-

4.2.3 Decision Tree Regression

The Decision Tree model is used to depict the relationships between variables, comparing actual and predicted tensile strength for each independent variable category. In Figure 4.2, the structure is evident, showcasing nodes and leaves, allowing us to observe and comment on influential variables in splitting nodes and determining the model's predictive path. The model considers key factors like printing speed, infill density, and layer thickness but not extrusion temperature until the fourth node. As a result, the model gives R^2 scores of 0.30, 0.30, and 0.48 for the datasets, respectively; these are unsatisfactory results, as seen in Table 3.2.

To see the effect of the parameters on the model, layer thickness and infill density demonstrate significant influence across all datasets, with layer thickness being particularly dominant in Dataset 1 and Dataset 2 in Figure 4.8. In contrast, bed temperature appears to have a minimal impact on the model's predictions.

The results of our study indicate that in Figure 4.3, the Decision Tree models exhibit significant overfitting across the datasets. For Dataset 1, the model shows a high R^2 score of 0.96 on the training set but drops to 0.30 on the test set. Similarly, for Dataset 2, the model has a training R^2 of 0.92 and a test R^2 of 0.30. In contrast, for Dataset 3, with a lower training R^2 of 0.74, the model shows relatively better generalization with a test R^2 of 0.48. These discrepancies highlight the models' tendency to overfit the training data, particularly in Datasets 1 and 2, indicating a need for further tuning to improve generalization to unseen data.

4.2.4 eXtreme Gradient Boosting (XGBoost) Regression

Finally, eXtreme Gradient Boosting (XGBoost) is applied to the datasets. XGBoost minimizes errors and prevents overfitting by using residuals and regularization techniques. As mentioned in Section 3.3.4: "Throughout the thesis, while the residuals may not be directly observable at each step, the model calculates them continuously in the background as part of its internal processing. Additionally, XGBoost incorporates regularization techniques to control the complexity of the trees. After a predefined number of iterations or when a stopping criterion is met, the model combines the predictions from all the trees to produce the final regression result."

A summary of the residuals of the model is accessible in Table 4.3, providing insights into the model's performance and facilitating informed adjustments for achieving even greater accuracy in regression predictions. The number of estimators is limited to 100 and 500; subsample 0.8 and 1.0; gamma 0, 1, 5; max depth 3, 4, 5; and learning rate 0.1 and 0.3 in the parameters, and the model was tuned with the best parameters by GridSearch for the datasets.

Table 4.3
Residuals table for the XGBoost model that used the 3rd dataset.

Index	Actual	Predicted	Residuals
0	33.67	33.545000	0.125000
1	11.00	25.750000	-14.750000
2	25.00	25.750000	-0.750000
3	56.39	51.318750	5.071250
4	36.80	39.966667	-3.166667
5	35.93	33.545000	2.385000
6	29.00	25.750000	3.250000
7	48.39	46.747500	1.642500
8	43.92	51.318750	-7.398750
9	12.00	25.750000	-13.750000
10	36.17	39.966667	-3.796667
11	47.21	46.747500	0.462500
12	24.00	25.750000	-1.750000
13	34.70	39.966667	-5.266667
14	22.00	25.750000	-3.750000
15	58.98	33.545000	25.435000
16	42.63	25.750000	16.880000
17	35.07	39.966667	-4.896667
18	35.87	33.545000	2.325000
19	49.67	46.747500	2.922500
20	18.00	25.750000	-7.750000
21	54.20	33.545000	20.655000

The XGBoost model application resulted in R^2 scores of 0.56, 0.58, and 0.59 for the datasets, respectively, as depicted in Figure 4.7. This signifies that the model can effectively fit 56-59 % of the variance in our target variable, emphasizing its stronger predictive capability compared to other models for the last dataset, as seen in Table 4.4.

However, the study shows that the XGBoost models are overfitting across all three datasets (Figure 4.3). The R^2 scores for the train sets are high (around 0.98-1.00), while the R^2 scores for the test set are significantly lower (around 0.56-0.59). This

suggests that the models perform well on the training data but struggle to generalize to new, unseen data. To accurately reflect the models' real-world performance, it is essential to emphasize the test set R^2 results in the project.

4.2.5 Evaluation of the Model Performances

Feature importance is utilized for Decision Tree Regression and XGBoost Regression models in Figure 4.8 for all three datasets. Infill density is consistently important across all features, with scores of 0.67, 0.67, and 0.55 for the Decision Tree model and 0.68, 0.68, and 0.51 for the XGBoost model, respectively.

The beeswarm plot is illustrated in Figure 4.9 for the SHAP value plots for an XGBoost model across three different datasets, labeled (a), (b), and (c). Each plot reveals the impact of features such as layer thickness, infill density, bed temperature (in one dataset), extrusion temperature, and printing speed on the model's prediction. Each dot in the plot represents the SHAP value for a specific feature for a single prediction, with the color indicating the feature value and it uses a color scale to indicate the magnitude of each feature's value, ranging from low (blue) to high (red). The distribution of SHAP values on these plots indicates the positive or negative influence of each feature on the model's output, offering insights into the model's behavior across different conditions and datasets.

The SHAP value plots demonstrate how various features influence the output of the XGBoost model across three datasets in Figure 4.9. For Dataset 1, infill density significantly impacts tensile strength, while layer thickness and printing speed also contribute. Dataset 2 introduces bed temperature, highlighting its notable influence along with sustained contributions from infill density and layer thickness. In Dataset 3, layer thickness becomes the dominant feature, significantly affecting model output, with infill density and printing speed playing supportive roles. These insights are crucial for optimizing 3D printing parameters to enhance product strength.

The evaluation of various machine learning models using K-fold method showcased performance levels. The K-fold validation, facilitated by GridSearchCV across three folds, examined 72 different hyperparameter combinations for the XGBoost regression model (Table 4.5).

Among the tested models, XGBoost consistently delivered the satisfactory performance across all datasets, achieving the higher R^2 values and demonstrating superior predictive accuracy. The Decision Tree also performed well in the first two datasets for K-Fold Cross Validation. In contrast, Support Vector Machine model exhibits moderate to lower predictive capabilities. Consequently, XGBoost stands out as the most effective model for these datasets, as evidenced by the K-Fold validation results.

Table 4.4
Machine learning models comparisons by R^2 results for the test set of three versions of datasets.

	1st Dataset	2nd Dataset	3rd Dataset	Success Level
Multiple Linear	0.69	0.73	0.37	Satisfactory for the short datasets
Support Vector	0.69	0.71	0.11	Satisfactory for the short datasets
Decision Tree	0.30	0.30	0.48	Unsatisfactory
XGBoosting	0.56	0.58	0.59	Satisfactory for the longer dataset

Table 4.5
K-Fold cross validations' R^2 results.

Model	1st Dataset	2nd Dataset	3rd Dataset
Multiple Linear	0.67	0.69	0.09
Support Vector	0.48	0.48	-0.25
Decision Tree	0.64	0.64	0.26
XGBoost	0.70	0.68	0.51

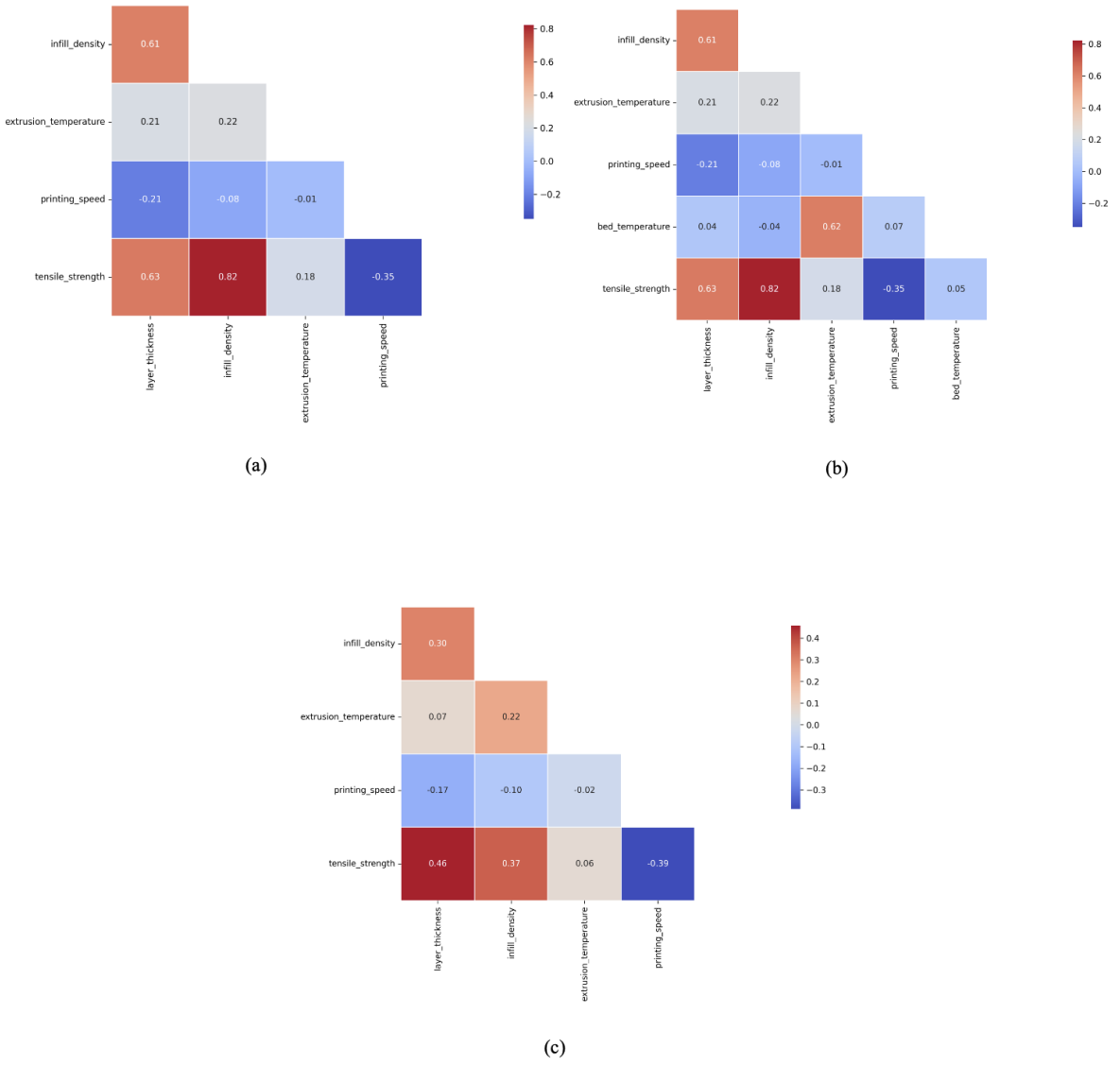

Figure 4.1 Correlation heatmap to evaluate the relationship strength between each other for the 1st (a), 2nd (b) and 3rd (c) datasets.

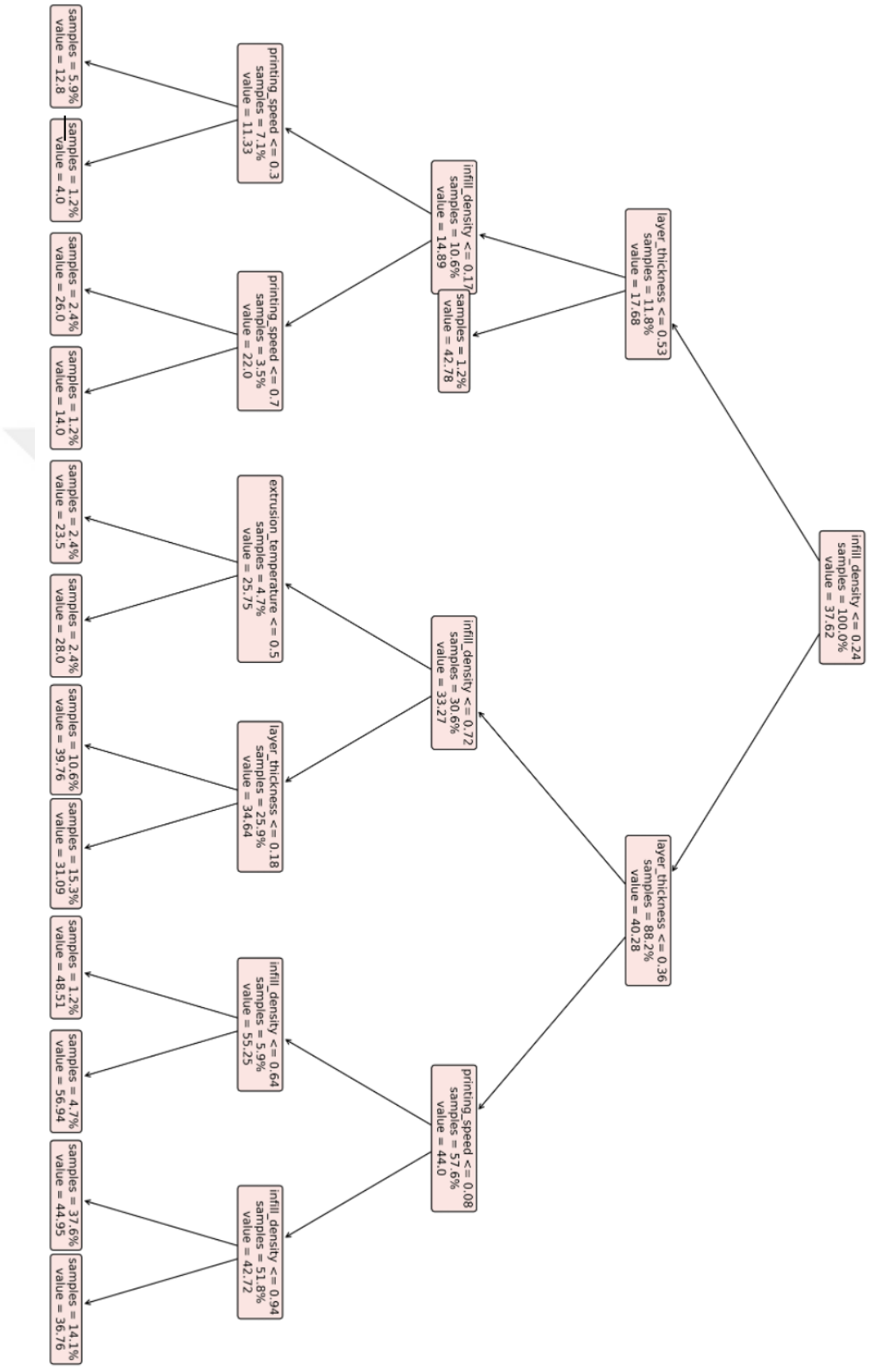

Figure 4.2 Illustration of the decision tree for the 3rd dataset, depicting a result of 0.48 obtained in the Decision Tree Regression task.

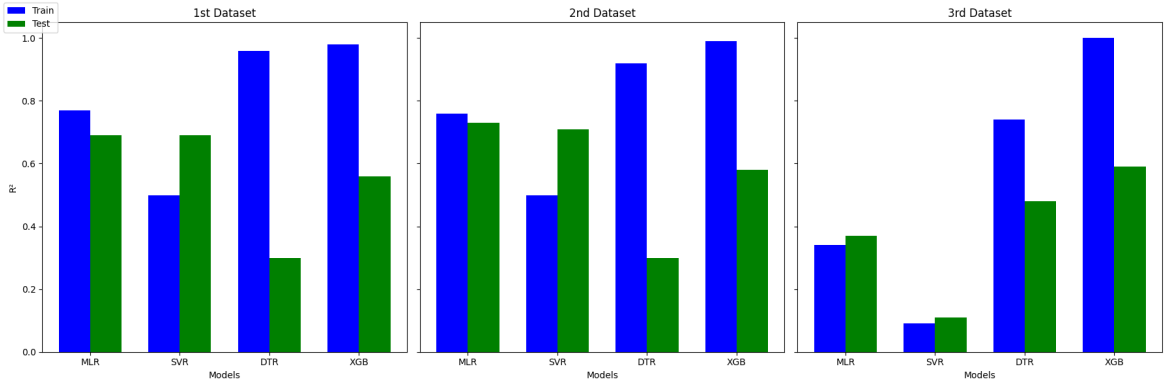

Figure 4.3 Comparison of R^2 results for train and test sets across different machine learning models (MLR, SVR, DTR, XGB) for three datasets. Each boxplot represents a different dataset, showing how each model performs in terms of R^2 scores for both training and testing phases.

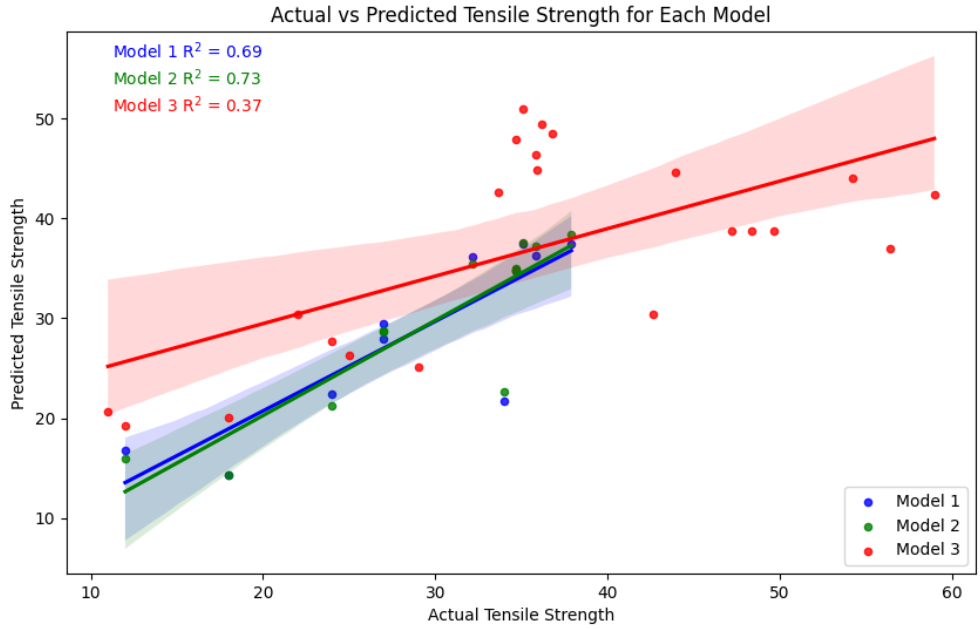

Figure 4.4 Comparison of Multiple Linear Regression (MLR) model results of three datasets with line of best fits.

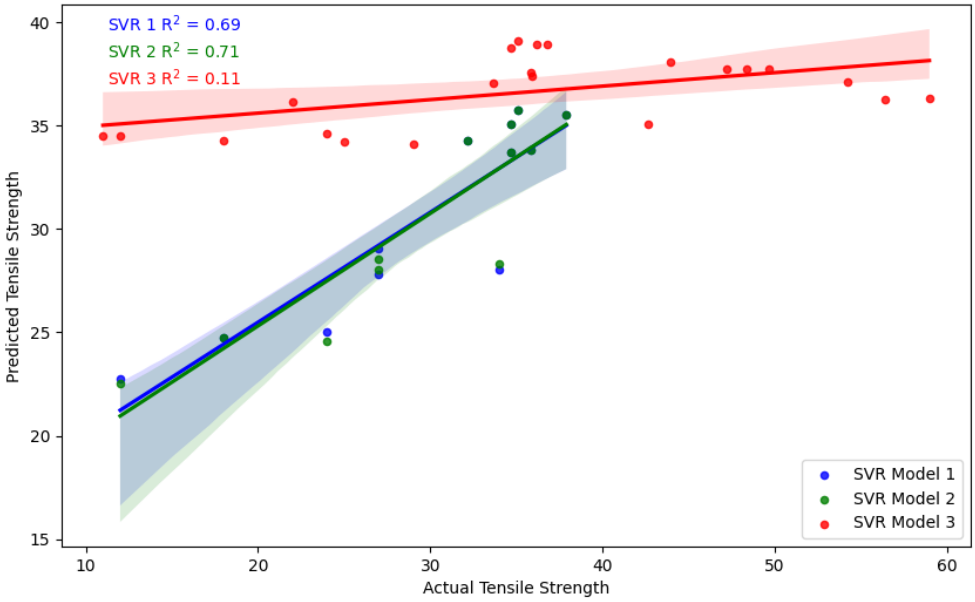

Figure 4.5 Comparison of Support Vector Regression (SVR) model results of three datasets with line of best fits.

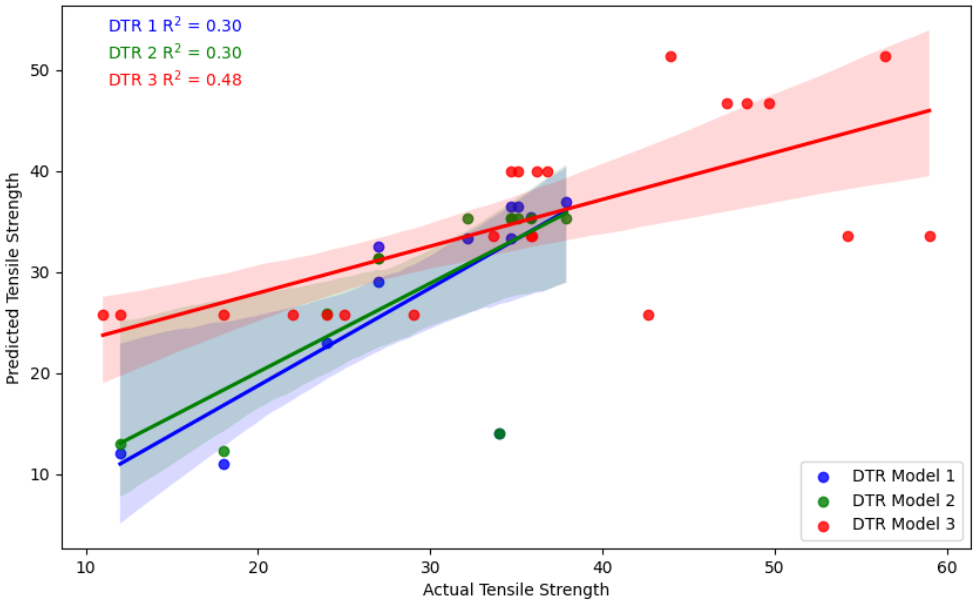

Figure 4.6 Comparison of Decision Tree Regression (DTR) model results of three datasets with line of best fits.

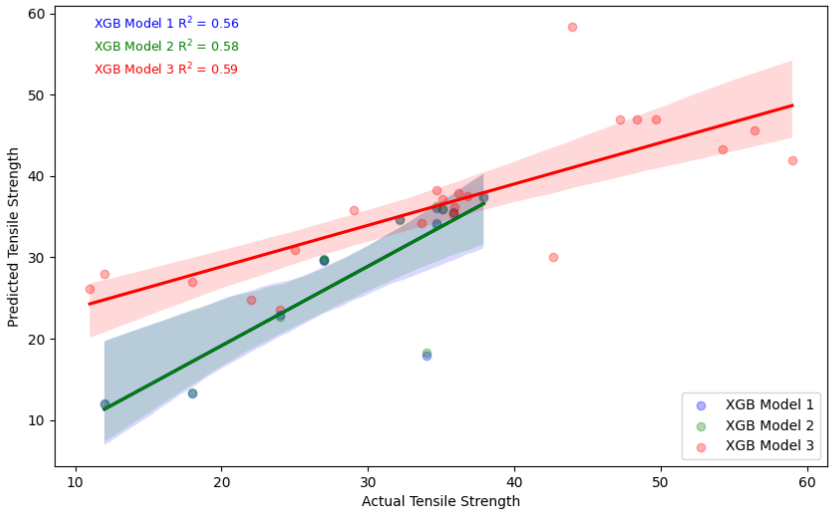

Figure 4.7 Comparison of XGBoost Regression model results of three datasets with line of best fits.

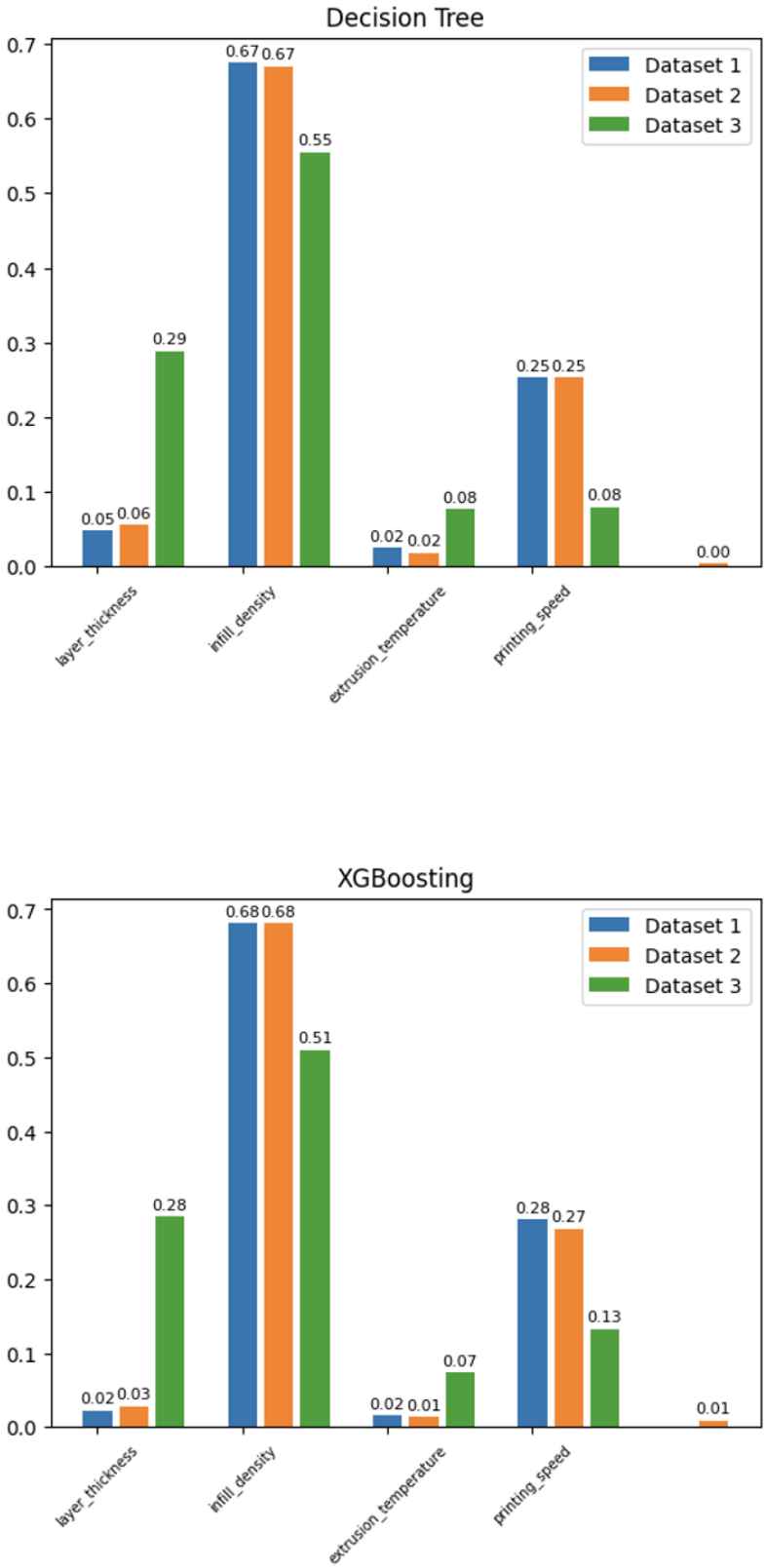

Figure 4.8 Feature importance analysis are illustrated for Decision Tree and XGBoosting regression models.

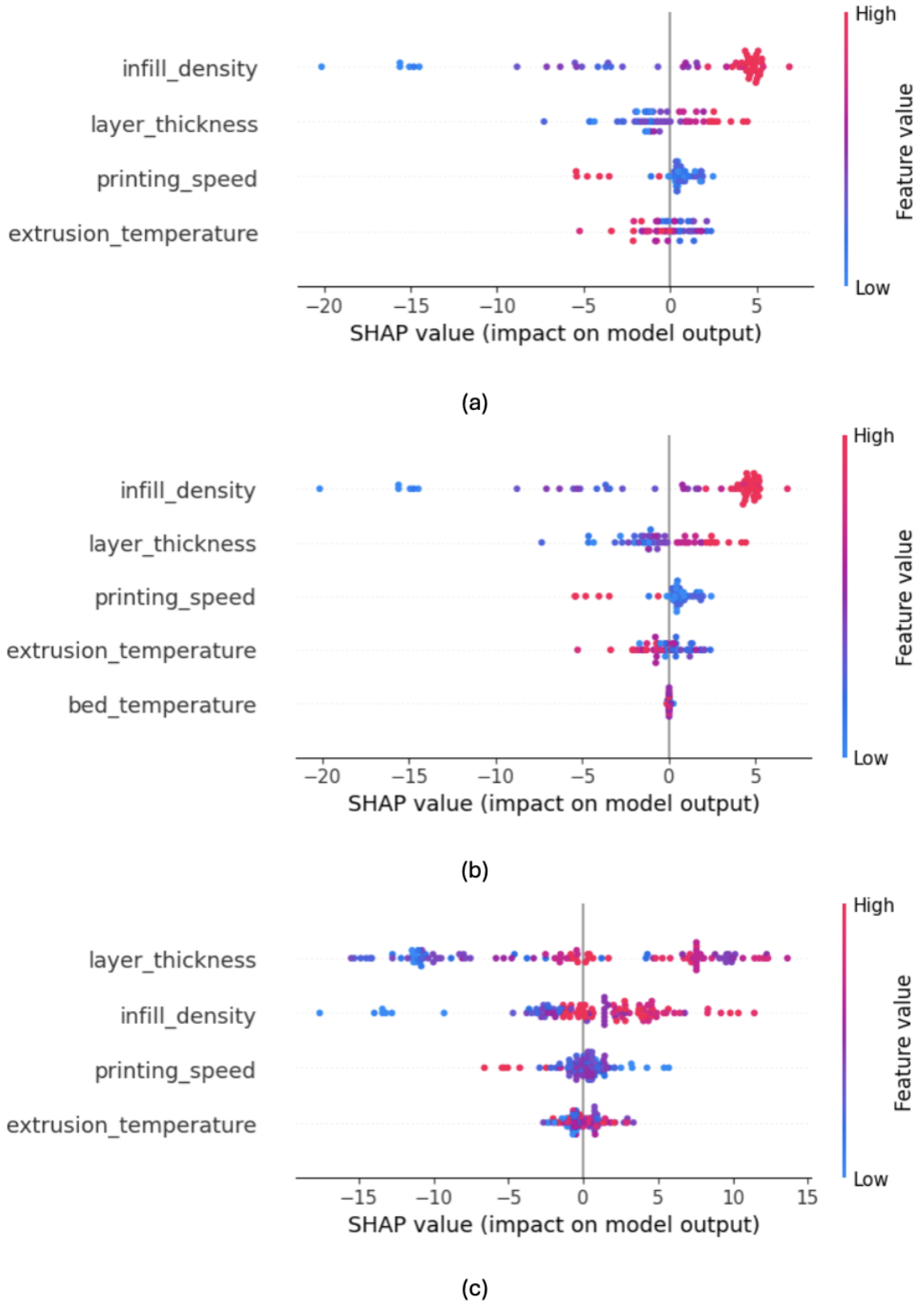

Figure 4.9 SHAP value (impact on model) with beeswarm plot for XGBoost model on the 1st (a), 2nd (b) and 3rd (c) datasets.

5. DISCUSSION AND FUTURE WORK

The integration of machine learning (ML) techniques into 3D printing has emerged as a promising field of study. Especially in predicting the mechanical and physical properties of printed materials based on parameters, the application of ML can significantly increase the efficiency and reliability of processes by optimizing parameters: layer thickness, printing speed, infill density, extrusion temperature, and bed temperature. This discussion section synthesizes findings from existing results and literature to highlight advances, challenges, and future directions in this field.

The machine learning models demonstrated varied performances across different datasets of 3D printing parameters, as detailed in Table 4.4. MLR and SVR yield more favorable outcomes with smaller datasets, and their performance improves when the dataset incorporates the bed temperature parameter. Conversely, Decision Tree and XGBoost Regression models excel with larger datasets, although the literature suggests that the XGBoost model is expected to perform well on smaller datasets due to its design principles (Table 4.4) [84].

In Section 4.1.3, Decision Tree Regression considered three out of the four independent variables, excluding extrusion temperature (Figure 4.2) until the fourth node. The reason might be that during the training process, the algorithm would determine that extrusion temperature did not significantly enhance the model's predictive performance, as decision trees can automatically identify and select the most informative features based on their effectiveness in splitting the data and reduce uncertainty in predicting the target variable [81].

When we evaluate the model performances with cross validation methods (K-Fold Cross), according to Tables 3.4 and 4.4, the XGBoost model shows consistent strength across all configurations, handling both the increase in parameters (as seen in the second dataset with five parameters) and the larger data volume (in the third

dataset with 107 rows) effectively. This suggests that XGBoost is well-suited for larger and more complex datasets due to its robust handling of higher-dimensional data.

In contrast, the Multiple Linear Regression and Support Vector Machine models, which performed adequately on the smaller datasets (58 rows), show a decline in performance on the larger dataset. This drop might be due to the models' limited capacity to manage the increased complexity and size without overfitting or underfitting, which are common challenges in scalable machine learning applications. Additionally, the decrease in performance can be attributed to the lack of a linear relationship between the data and tensile strength [16],[91].

The Decision Tree model exhibited lower performance across the first two datasets but performed relatively well on the third dataset. This suggests potential issues with its setup or its fundamental suitability to the type of data and tasks at hand. Despite the variation in size or number of parameters, the improved performance on the third dataset indicates that the model may require significant tuning or reconsideration of its application to these specific datasets [92], [93].

The analysis of both the train set and the specific test set offers valuable insights into how different machine learning models perform in optimizing 3D printing parameters. Key findings from the broader dataset confirm that complex models like XGBoost and Decision Tree handle large, detailed datasets better. These models also proved effective in the test set, which was designed to mimic real-world conditions with varied and unpredictable data.

The test set results particularly highlight XGBoost's strength. This model not only met but often surpassed performance expectations in real-world scenarios, showcasing its potential as a reliable tool for the 3D printing industry where conditions can vary greatly. Conversely, more straightforward models like Multiple Linear Regression and Support Vector Regression performed well with smaller, controlled datasets but were less effective in the test set, indicating limitations in their application for more complex tasks.

Moreover, the test set revealed the adaptability of models like the Decision Tree. Although this model showed inconsistent results initially, it managed unseen and complex data effectively in the test set. This adaptability is key for models used in dynamic industries like 3D printing, suggesting that even if some models need initial adjustments, their ability to handle new data without extensive retraining is critical.

In summary, the test set not only supports the findings from the larger dataset but also underscores the importance of choosing and fine-tuning machine learning models that can consistently perform well in theoretical and practical settings. Achieving this balance is crucial for improving the efficiency and quality of 3D printed materials through machine learning.

5.1 Parameter Effects on the Model Results

Each parameter and dataset have unique effects on the model results according to their interactions with other parameters, and this changes with both the size of the datasets and the parameters. In this section, the parameter effect is discussed, and as discussed in the previous section, the possibility of overfitting in smaller datasets should be considered while evaluating the assumptions.

1. Layer Thickness: It is strongly correlated with tensile strength in all three datasets (Figure 4.1). This correlation suggests that thicker layers improve the bond between layers and leading to fewer structural weaknesses such as gaps [8].

   In Support Vector regression model, it has the highest linear kernel coefficients for each dataset in Table 4.2. Also, it comes forward in feature importance, especially for the third dataset in Decision Tree and XGBoost (Figure 4.8) regression models. The parameter shows a significant impact in Decision Tree Regression model for the 3rd dataset, which is the parameter for second level branches in Figure 4.2.

   The SHAP value plots (Figure 4.9) for the XGBoost model on all three datasets illustrate the importance of the features. The effect of layer thickness on model

output differs across the plots. In plot a, layer thickness has minimal impact, suggesting it's not crucial for that model. However, plot b indicates that thicker layers slightly enhance the output and thinner layers reduce it, showing a mild positive correlation with tensile strength. In plot c, the relationship is more pronounced, where thicker layers notably improve the output, suggesting that optimal layer thickness can significantly support the bonding between layers and improve the structural integrity and tensile strength of the print. This underscores the importance of optimizing layer thickness to enhance the structural integrity of 3D-printed objects [8],[94].

2. Infill Density: It has a strong positive correlation with tensile strength in all three datasets, similarly in layer thickness (Figure 4.1). There is no interpretable result for MLR, yet we can see that it has positive linear kernel coefficients in SVR and is in the second place between parameters according to Table 4.2. It also comes forward in feature importance for both Decision Tree and XGBoost regression models with the highest analysis results and is the main parameter for the first node in the decision tree in Figure 4.2 [95],[96]. Lastly, the provided SHAP beeswarm plots (Figure 4.9) illustrate how infill density affects the model's predictions for tensile strength. Across all three plots, there is a consistent strong positive correlation between high infill density and the model output, indicating its significant impact on tensile strength. High infill density values increase the model output, indicating that a denser internal structure results in stronger, more durable prints [97]. Although plot c shows a slightly less pronounced effect, the positive correlation remains clear, emphasizing that increasing infill density generally improves the tensile strength of 3D-printed objects.

3. Extrusion Temperature: This parameter shows poor correlation (Figure 4.1) and poor results in feature importance analyses compared to other parameters (Figure 4.8). As seen in Figure 4.6, extrusion temperature is not appeared until the forth node.

   The analysis of the extrusion temperature parameter from the SHAP value plots reveals that its effect on the model's output is complex and less predictable compared to printing speed in Figure 4.9. Lower extrusion temperatures consistently

show a negative impact, likely due to inadequate material flow and bonding. In contrast, higher extrusion temperatures exhibit mixed effects, sometimes beneficial and other times detrimental, depending on other factors i.e. printing speed and bed temperature [98],[99].

4. Printing Speed: This parameter shows a strong negative correlation with tensile strength (Figure 4.1). Feature importance analysis (Figure 4.8) shows values ranging from 0.08 to 0.25 for the Decision Tree model and 0.13 to 0.28 for the XGBoost model. Higher printing speeds reduce production time but result in poorer performance as the nozzle moves too quickly to fine-tune the object, leading to lower tensile strength [28]. As a support, SHAP value plots (Figure 4.9) indicate that higher printing speeds generally have a negative impact on the model's output. Additionally, the parameter shows significant importance in the Decision Tree model, with its place in the third node (Figure 4.2).

5. Bed Temperature: Bed temperature is negatively correlated with tensile strength (Figure 4.1). Including this parameter slightly improves model performance in the second dataset compared to the first dataset, which lacks this parameter (Table 4.4). Feature importance figures (Figure 4.8) show its importance is nearly zero. SHAP analysis (Figure 4.9, plot b) indicates low bed temperatures significantly decrease model output, while high values have a slight positive impact [100]. An optimal bed temperature ensures proper adhesion, reduces warping, and improves layer bonding, resulting in stronger prints [101]. However, its impact on ML model performance in our study is low. The reason for this could be that the variations in bed temperature within the tested range do not significantly affect the overall structural integrity of the prints [102]. Additionally, other factors like printing speed, infill density, extrusion temperature, and layer thickness might play more dominant roles in determining tensile strength, overshadowing the influence of bed temperature [103]. This could explain why the bed temperature parameter shows minimal importance in feature analysis and SHAP values.

In conclusion, the application of ML in 3D printing holds significant promise for the optimization of printing parameters and the prediction of material properties.

However, realizing this potential requires overcoming challenges related to data quality, model complexity, and computational resources. Future research should focus on developing standardized datasets, improving data collection methods, increasing the number of parameters, and exploring new machine learning algorithms tailored to the specific needs of additive manufacturing. Collaboration between materials scientists, engineers, and data scientists will be key to advancing this field and taking full advantage of the capabilities of machine learning in 3D printing technologies.

In our next steps for this thesis, we plan to create a simple interface and make it more useful and easy to use. This tool will allow anyone, from scientists to hobbyists, to quickly choose 3D printing settings and get instant advice on the strength and other qualities of their prints, making cutting-edge predictions available to everyone. We also see the chance to turn this into a business by launching a company that offers tailored advice to companies using 3D printing in sectors especially for healthcare (for prosthetic manufacturing), aerospace (for parts), and fashion (for unique accessories), helping them get the best results from their printing. Adding more features to make the platform better is possible, such as predicting how well materials will work with biological systems or how long they will last in different environments. Partnering with 3D printer manufacturers can allow the software to work directly with printers, making the printing process smoother and more efficient using the latest data. This comprehensive strategy aims to take the thesis to the cutting edge of 3D printing technology, paving the way for more efficient, environmentally friendly, and personalized production.

6. CONCLUSION

This thesis demonstrates the significant impact of machine learning on the development of 3D printing techniques in the field of biomaterials. By examining how different printing parameters such as extrusion temperature, layer thickness, bed temperature, infill density, and printing speed affect the strength of printed materials, this study highlights the advantages of using predictive models to enhance the printing workflow.

The research involved analysis of a dataset containing 107 observations from five published studies focused on evaluating four machine learning models: Multiple Linear, Decision Tree, Support Vector, and XGBoost. The findings indicated that the XGBoost model was particularly effective, producing the most accurate predictions with values of 0.56, 0.58, and 0.59 R^2; this shows that it can successfully manage complex data relationships better than other tested models.

In conclusion, the findings of this thesis confirm that the application of machine learning to 3D printing of biomaterials is a practical and valuable innovation. By improving the development and use of materials, it paves the way for further research in this field and expands the scope of artificial intelligence applications in materials science. As machine learning continues to advance, it is poised to become an integral part of developing new and more effective methods for manufacturing materials.

7. SUPPLEMENTARY DATA

Table 7.1
Parameters for 3D Printing and Tensile Strength Values of PLA. All versions of the datasets and model applications scripts are available at: *kaggle.com/sedaserttrk*.

No	Layer Thickness (mm)	Infill Density (%)	Extrusion Temperature (°C)	Printing Speed (mm/s)	Tensile Strength (MPa)
1	0.02	40	200	40	24
2	0.02	10	205	40	12
3	0.02	10	210	40	14
4	0.02	70	215	40	27
5	0.02	40	220	40	25
6	0.06	90	200	60	7
7	0.06	40	205	60	23
8	0.06	30	210	60	26
9	0.06	80	215	60	33
10	0.06	50	220	60	29
11	0.1	50	200	120	11
12	0.1	40	205	120	12
13	0.1	50	210	120	18
14	0.1	90	215	120	34
15	0.1	30	220	120	14
16	0.15	80	200	60	33
17	0.15	50	205	60	24
18	0.15	30	210	60	26
19	0.15	40	215	60	22
20	0.15	10	220	60	4
21	0.2	60	200	40	28
22	0.2	20	205	40	14

REFERENCES

1. Lee, J., "A 3d food printing process for the new normal era: A review," *Processes*, Vol. 9, p. 1495, August 2021.

2. Shackelford, J. F., *Introduction to Materials Science for Engineers*, Pearson, 2015.

3. Ranakoti, L., B. Gangil, S. K. Mishra, T. Singh, S. Sharma, R. Ilyas, and S. El-Khatib, "Critical review on polylactic acid: Properties, structure, processing, biocomposites, and nanocomposites," *Materials*, Vol. 15, p. 4312, June 2022.

4. Thomas, L., and O. Eric, "A beginner's guide to deep learning." `https://www.enthought.com/blog/a-beginners-guide-to-deep-learning/`, 2024. Accessed: 2024-02-13.

5. Hastie, T., R. Tibshirani, and J. Friedman, *The Elements of Statistical Learning: Data Mining, Inference, and Prediction*, Springer, 2nd ed., 2009. Available: `https://web.stanford.edu/~hastie/ElemStatLearn/`.

6. Carvill, J., *Strengths of materials*, pp. 1–55. Elsevier, 1993.

7. Tura, A. D., H. G. Lemu, L. E. Melaku, and H. B. Mamo, *Impact of FDM 3D Printing Parameters on Compressive Strength and Printing Weight of PLA Components*, pp. 495–504. Springer Nature Singapore, 2023.

8. Shergill, K., Y. Chen, and S. Bull, "An investigation into the layer thickness effect on the mechanical properties of additively manufactured polymers: Pla and abs," *The International Journal of Advanced Manufacturing Technology*, Vol. 126, pp. 3651–3665, April 2023.

9. Kumar, M. S., M. U. Farooq, N. S. Ross, C.-H. Yang, V. Kavimani, and A. A. Adediran, "Achieving effective interlayer bonding of pla parts during the material extrusion process with enhanced mechanical properties," *Scientific Reports*, Vol. 13, April 2023.

10. Ansari, S., and A. B. Nassif, "A comprehensive study of regression analysis and the existing techniques," in *2022 Advances in Science and Engineering Technology International Conferences (ASET)*, pp. 1–10, 2022.

11. "Introduction to boosted trees, xgboost 2.0.3 documentation." `https://xgboost.readthedocs.io/en/stable/tutorials/model.html`, 2024. Accessed: 2024-01-31.

12. Nasiri, S., and M. R. Khosravani, "Machine learning in predicting mechanical behavior of additively manufactured parts," *Journal of Materials Research and Technology*, Vol. 14, pp. 1137–1153, September 2021.

13. Zadpoor, A. A., "Mechanical performance of additively manufactured meta-biomaterials," *Acta Biomaterialia*, Vol. 85, pp. 41–59, February 2019.

14. Liu, Y., T. Zhao, W. Ju, and S. Shi, "Materials discovery and design using machine learning," *Journal of Materiomics*, Vol. 3, pp. 159–177, September 2017.

15. Goh, G. D., S. L. Sing, and W. Y. Yeong, "A review on machine learning in 3d printing: applications, potential, and challenges," *Artificial Intelligence Review*, Vol. 54, pp. 63–94, July 2020.

16. Ege, D., S. Sertturk, B. Acarkan, and A. Ademoglu, "Machine learning models to predict the relationship between printing parameters and tensile strength of 3d poly (lactic acid) scaffolds for tissue engineering applications," *Biomedical Physics Engineering Express*, Vol. 9, p. 065014, October 2023.

17. Egan, P. F., "Design for additive manufacturing: Recent innovations and future directions," *Designs*, Vol. 7, p. 83, June 2023.

18. Williams, R. J., and S. L. Sing, *3D Printing*. CRC Press, February 2023.

19. Chia, H. N., and B. M. Wu, "Recent advances in 3d printing of biomaterials," *Journal of Biological Engineering*, Vol. 9, March 2015.

20. Vukicevic, M., B. Mosadegh, J. K. Min, and S. H. Little, "Cardiac 3d printing and its future directions," *JACC: Cardiovascular Imaging*, Vol. 10, pp. 171–184, February 2017.

21. Ota, H., S. Emaminejad, Y. Gao, A. Zhao, E. Wu, S. Challa, K. Chen, H. M. Fahad, A. K. Jha, D. Kiriya, W. Gao, H. Shiraki, K. Morioka, A. R. Ferguson, K. E. Healy, R. W. Davis, and A. Javey, "Application of 3d printing for smart objects with embedded electronic sensors and systems," *Advanced Materials Technologies*, Vol. 1, March 2016.

22. "Every 3d printer part explained (2023 update) - 3dsourced." `https://www.3dsourced.com/guides/3d-printer-parts/`, 2024. Accessed: 2024-02-11.

23. Mateti, T., S. Jain, L. Ananda Shruthi, A. Laha, and G. Thakur, *An overview of the advances in the 3D printing technology*, pp. 1–37. Elsevier, 2023.

24. Mushtaq, R. T., A. Iqbal, Y. Wang, M. Rehman, and M. I. Petra, "Investigation and optimization of effects of 3d printer process parameters on performance parameters," *Materials*, Vol. 16, p. 3392, April 2023.

25. Noh, H., K. Park, and H. W. Jeon, "Selection of infill parameters considering their effects on operational and mechanical performance for material extrusion of cfr-peek," *Rapid Prototyping Journal*, Vol. 29, pp. 1471–1485, April 2023.

26. Yu, C., and J. Jiang, "A perspective on using machine learning in 3d bioprinting," *International Journal of Bioprinting*, Vol. 6, p. 253, January 2020.

27. Tanveer, M. Q., G. Mishra, S. Mishra, and R. Sharma, "Effect of infill pattern and infill density on mechanical behaviour of fdm 3d printed parts: A current review," *Materials Today: Proceedings*, Vol. 62, pp. 100–108, 2022.

28. Ansari, A. A., and M. Kamil, "Effect of print speed and extrusion temperature on properties of 3d printed pla using fused deposition modeling process," *Materials Today: Proceedings*, Vol. 45, pp. 5462–5468, 2021.

29. "3d printing concepts and 3d printer parts - leapfrog 3d printers." `https://www.lpfrg.com/guides/3d-printing-concepts-and-3d-printer-parts/`, 2024. Accessed: 2024-04-02.

30. Mamo, H. B., M. Adamiak, and A. Kunwar, "3d printed biomedical devices and their applications: A review on state-of-the-art technologies, existing challenges, and future perspectives," *Journal of the Mechanical Behavior of Biomedical Materials*, Vol. 143, p. 105930, July 2023.

31. Trenfield, S. J., A. Awad, A. Goyanes, S. Gaisford, and A. W. Basit, "3d printing pharmaceuticals: Drug development to frontline care," *Trends in Pharmacological Sciences*, Vol. 39, pp. 440–451, May 2018.

32. Mitchell, A., U. Lafont, and Mart, "Additive manufacturing: A review of 4d printing and future applications," *Additive Manufacturing*, Vol. 24.

33. Ramezani, M., and Z. Mohd Ripin, "4d printing in biomedical engineering: Advancements, challenges, and future directions," *Journal of Functional Biomaterials*, Vol. 14, p. 347, June 2023.

34. "Materials science | definition, types, study, facts | britannica." `https://www.britannica.com/technology/materials-science`, 2024. Accessed: 2024-03-12.

35. Callister, W. D., and D. G. Rethwisch, *Materials Science and Engineering: An Introduction*, John Wiley Sons, 2018.

36. Zhuravkov, M., Y. Lyu, and E. Starovoitov, *Material and Solid Mechanical Characteristics (Properties)*, pp. 51–62. Springer Nature Singapore, 2023.

37. Meyers, M. A., and K. K. Chawla, *Mechanical Behavior of Materials*, Cambridge University Press, 2009.

38. Qu, J., L. Ouyang, C.-c. Kuo, and D. C. Martin, "Stiffness, strength and adhesion characterization of electrochemically deposited conjugated polymer films," *Acta Biomaterialia*, Vol. 31, pp. 114–121, February 2016.

39. Santos, P. F., M. Niinomi, H. Liu, K. Cho, M. Nakai, Y. Itoh, T. Narushima, and M. Ikeda, "Fabrication of low-cost beta-type ti–mn alloys for biomedical applications by metal injection molding process and their mechanical properties," *Journal of the Mechanical Behavior of Biomedical Materials*, Vol. 59, pp. 497–507, June 2016.

40. Bergstrom, J. S., and D. Hayman, "An overview of mechanical properties and material modeling of polylactide (pla) for medical applications," *Annals of Biomedical Engineering*, Vol. 44, pp. 330–340, September 2015.

41. Davachi, S. M., and B. Kaffashi, "Polylactic acid in medicine," *Polymer-Plastics Technology and Engineering*, Vol. 54, pp. 944–967, January 2015.

42. Hamad, K., M. Kaseem, H. W. Yang, F. Deri, and Y. G. Ko, "Properties and medical applications of polylactic acid: A review," *Express Polymer Letters*, Vol. 9, no. 15, pp. 435–455, 2015.

43. Li, G., M. Zhao, F. Xu, B. Yang, X. Li, X. Meng, L. Teng, F. Sun, and Y. Li, "Synthesis and biological application of polylactic acid," *Molecules*, Vol. 25, p. 5023, October 2020.

44. Bikiaris, N. D., I. Koumentakou, C. Samiotaki, D. Meimaroglou, D. Varytimidou, A. Karatza, Z. Kalantzis, M. Roussou, R. D. Bikiaris, and G. Z. Papageorgiou, "Recent advances in the investigation of poly(lactic acid) (pla) nanocomposites: Incorporation of various nanofillers and their properties and applications," *Polymers*, Vol. 15, p. 1196, February 2023.

45. Liu, Z., Y. Wang, B. Wu, C. Cui, Y. Guo, and C. Yan, "A critical review of fused deposition modeling 3d printing technology in manufacturing polylactic acid parts," *The International Journal of Advanced Manufacturing Technology*, Vol. 102, pp. 2877–2889, February 2019.

46. Sandanamsamy, L., J. Mogan, N. A. Halim, W. S. W. Harun, K. Kadirgama, and D. Ramasamy, "A review on 3d printing bio-based polymer composite," *IOP Conference Series: Materials Science and Engineering*, Vol. 1078, p. 012031, February 2021.

47. Gonzalez-Rodriguez, L., S. Perez-Davila, R. Lama, M. Lopez-Alvarez, J. Serra, B. Novoa, A. Figueras, and P. Gonzalez, "3d printing of pla:cap:go scaffolds for bone tissue applications," *RSC Advances*, Vol. 13, no. 23, pp. 15947–15959, 2023.

48. Perez-Davila, S., L. Gonzalez-Rodriguez, Lama, A. L. Oliveira, J. Serra, B. Novoa, A. Figueras, and P. Gonzalez, "3d-printed pla medical devices: Physicochemical changes and biological response after sterilisation treatments," *Polymers*, Vol. 14, p. 4117, October 2022.

49. Turing, A. M., "I.—computing machinery and intelligence," *Mind*, Vol. LIX, pp. 433–460, October 1950.

50. Rosenblatt, F., "Principles of neurodynamics. perceptrons and the theory of brain mechanisms," *American Journal of Psychology*, Vol. 76, p. 705, 1963.

51. Rumelhart, D. E., G. E. Hinton, and R. J. Williams, "Learning representations by back-propagating errors," *Nature*, Vol. 323, pp. 533–536, 1986.

52. Cortes, C., and V. Vapnik, "Support-vector networks," *Machine Learning*, Vol. 20, pp. 273–297, September 1995.

53. Jordan, M. I., and T. M. Mitchell, "Machine learning: Trends, perspectives, and prospects," *Science*, Vol. 349, pp. 255–260, July 2015.

54. "Machine learning, explained | mit sloan." `https://mitsloan.mit.edu/ideas-made-to-matter/machine-learning-explained`, 2024. Accessed: 2024-03-14.

55. Muller, A. C., and S. Guido, *Introduction to Machine Learning with Python*, O'Reilly Media, Inc., 2016.

56. Libbrecht, M. W., and W. S. Noble, "Machine learning applications in genetics and genomics," *Nature Reviews Genetics*, Vol. 16, pp. 321–332, May 2015.

57. Wang, "Scientific discovery in the age of artificial intelligence," *Nature*, Vol. 620, pp. 47–60, 2023.

58. Jatti, V. S., M. S. Sapre, A. V. Jatti, N. K. Khedkar, and V. S. Jatti, "Mechanical properties of 3d-printed components using fused deposition modeling: Optimization using the desirability approach and machine learning regressor," *Applied System Innovation*, Vol. 5, p. 112, November 2022.

59. Hikmat, M., S. Rostam, and Y. M. Ahmed, "Investigation of tensile property-based taguchi method of pla parts fabricated by fdm 3d printing technology," *Results in Engineering*, Vol. 11, p. 100264, September 2021.

60. Gao, G., F. Xu, and J. Xu, "Parametric optimization of fdm process for improving mechanical strengths using taguchi method and response surface method: A comparative investigation," *Machines*, Vol. 10, p. 750, August 2022.

61. "3d printer dataset for mechanical engineers." `https://www.kaggle.com/datasets/afumetto/3dprinter/data`, 2024. Accessed: 2024-04-04.

62. Popescu, D., A. Zapciu, C. Amza, F. Baciu, and R. Marinescu, "Fdm process parameters influence over the mechanical properties of polymer specimens: A review," *Polymer Testing*, Vol. 69, pp. 157–166, August 2018.

63. Lanzotti, A., M. Grasso, G. Staiano, and M. Martorelli, "The impact of process parameters on mechanical properties of parts fabricated in pla with an open-source 3-d printer," *Rapid Prototyping Journal*, Vol. 21, pp. 604–617, August 2015.

64. Ivorra Martinez, J., L. Quiles Carrillo, D. Lascano, S. Ferrandiz Bou, and T. Boronat Vitoria, "Effect of infill parameters on mechanical properties in additive manufacturing," *DYNA*, Vol. 95, pp. 412–417, July 2020.

65. Ahn, S., M. Montero, D. Odell, S. Roundy, and P. K. Wright, "Anisotropic material properties of fused deposition modeling abs," *Rapid Prototyping Journal*, Vol. 8, pp. 248–257, October 2002.

66. Wang, S., Y. Ma, Z. Deng, S. Zhang, and J. Cai, "Effects of fused deposition modeling process parameters on tensile, dynamic mechanical properties of 3d printed polylactic acid materials," *Polymer Testing*, Vol. 86, p. 106483, June 2020.

67. Giri, J., A. Chiwande, Y. Gupta, C. Mahatme, and P. Giri, "Effect of process parameters on mechanical properties of 3d printed samples using fdm process," *Materials Today: Proceedings*, Vol. 47, pp. 5856–5861, 2021.

68. "What is numpy? numpy v1.26 manual." `https://numpy.org/doc/stable/user/whatisnumpy.html`, 2024. Accessed: 2024-03-15.

69. "Pandas documentation, pandas 2.2.1 documentation." `https://pandas.pydata.org/docs/`, 2024. Accessed: 2024-03-15.

70. "Scikit-learn: machine learning in python, scikit-learn 1.4.1 documentation." `https://scikit-learn.org/stable/`, 2024. Accessed: 2024-03-15.

71. "Matplotlib, visualization with python." `https://matplotlib.org/`, 2024. Accessed: 2024-03-15.

72. "Seaborn: statistical data visualization, seaborn 0.13.2 documentation." `https://seaborn.pydata.org/`, 2024. Accessed: 2024-03-15.

73. Bishop, C. M., *Pattern Recognition and Machine Learning*, Springer New York, NY, 2006.

74. Schölkopf, B., and A. J. Smola, *Learning with Kernels: Support Vector Machines, Regularization, Optimization, and Beyond*, MIT Press, 2002.

75. "What is normalization in machine learning? a comprehensive guide to data rescaling | datacamp." `https://www.datacamp.com/tutorial/normalization-in-machine-learning`, 2024. Accessed: 2024-06-23.

76. Neter, J., M. H. Kutner, C. J. Nachtsheim, and W. Wasserman, *Applied Linear Statistical Models*, McGraw-Hill Irwin, 1996.

77. "Applied regression analysis—a research tool," *Technometrics*, Vol. 41, pp. 82–82, February 1999.

78. Geron, A., *Hands-On Machine Learning with Scikit-Learn, Keras, and TensorFlow*, O'Reilly Media, Inc., 2019.

79. Smola, A. J., and B. Schölkopf, "A tutorial on support vector regression," *Statistics and Computing*, Vol. 14, no. 3, pp. 199–222, 2004.

80. "Decision trees - ibm documentation." `https://www.ibm.com/docs/en/db2/11.5?topic=building-decision-trees`, 2024. Accessed: 2024-01-26.

81. Breiman, L., J. H. Friedman, R. A. Olshen, and C. J. Stone, *Classification and Regression Trees*, Wadsworth, 1984.

82. Friedman, J. H., "Greedy function approximation: A gradient boosting machine," *The Annals of Statistics*, Vol. 29, pp. 1189–1232, October 2001.

83. Bentejac, C., A. Csorgo, and G. Martinez-Munoz, "A comparative analysis of gradient boosting algorithms," *Artificial Intelligence Review*, Vol. 54, pp. 1937–1967, August 2020.

84. Chen, T., and C. Guestrin, "Xgboost: A scalable tree boosting system," *In Proceedings of the 22nd ACM SIGKDD International Conference on Knowledge Discovery and Data Mining*, Vol. Not available, pp. 785–794, August 2016.

85. Nielsen, D., "Tree boosting with xgboost - why does xgboost win "every" machine learning competition?," Master's thesis, Norwegian University of Science and Technology, 2016.

86. Deisenroth, M. P., *Mathematics for Machine Learning*, Cambridge University Press, 2020.

87. "Seaborn.heatmap, seaborn 0.13.2 documentation." `https://seaborn.pydata.org/generated/seaborn.heatmap.html`, 2024. Accessed: 2024-04-03.

88. Kaneko, H., "Interpretation of machine learning models for data sets with many features using feature importance," *ACS Omega*, Vol. 8, pp. 23218–23225, June 2023.

89. Lundberg, S. M., and S.-I. Lee, "A unified approach to interpreting model predictions," in *Advances in Neural Information Processing Systems 30* (Guyon, I., U. V. Luxburg, S. Bengio, H. Wallach, R. Fergus, S. Vishwanathan, and R. Garnett, eds.), pp. 4765–4774, Curran Associates, Inc., 2017.

90. "An introduction to shap values and machine learning interpretability | datacamp." `https://www.datacamp.com/tutorial/introduction-to-shap-values-machine-learning-interpretability`, 2024. Accessed: 2024-05-16.

91. Maulud, D. H., and A. Abdulazeez, "A review on linear regression comprehensive in machine learning," 2020.

92. Zhu, L., G. Liu, S. Lv, D. Chen, Z. Chen, and X. Li, "An intelligent boosting and decision-tree-regression-based score prediction (bdtr-sp) method in the reform of tertiary education teaching," *Information*, Vol. 14, p. 317, may 2023.

93. "sklearn.tree.decisiontreeregressor — scikit-learn 1.4.2 documentation." `https://scikit-learn.org/stable/modules/generated/sklearn.tree.DecisionTreeRegressor.html`, 2024. Accessed: 2024-05-16.

94. Saniman, M. N. F., M. H. M Hashim, K. A. Mohammad, K. A. Abd Wahid, W. M. Wan Muhamad, and N. H. Noor Mohamed, "Tensile characteristics of low density infill patterns for mass reduction of 3d printed polylactic parts," *International Journal of Automotive and Mechanical Engineering*, Vol. 17, p. 7927–7934, July 2020.

95. Fernandez-Vicente, M., W. Calle, S. Ferrandiz, and A. Conejero, "Effect of infill parameters on tensile mechanical behavior in desktop 3d printing," *3D Printing and Additive Manufacturing*, Vol. 3, p. 183–192, sep 2016.

96. Rismalia, M., S. C. Hidajat, I. G. R. Permana, B. Hadisujoto, M. Muslimin, and F. Triawan, "Infill pattern and density effects on the tensile properties of 3d printed pla material," *Journal of Physics: Conference Series*, Vol. 1402, p. 044041, December 2019.

97. Rodriguez-Panes, A., J. Claver, and A. Camacho, "The influence of manufacturing parameters on the mechanical behaviour of pla and abs pieces manufactured by fdm: A comparative analysis," *Materials*, Vol. 11, p. 1333, August 2018.

98. Vidakis, N., M. Petousis, N. Mountakis, A. Moutsopoulou, and E. Karapidakis, "Energy consumption vs. tensile strength of poly[methyl methacrylate] in material extrusion 3d printing: The impact of six control settings," *Polymers*, Vol. 15, p. 845, feb 2023.

99. Costanzo, A., R. Spotorno, M. V. Candal, M. M. Fernández, A. J. Müller, R. S. Graham, D. Cavallo, and C. McIlroy, "Residual alignment and its effect on weld strength in material-extrusion 3d-printing of polylactic acid," *Additive Manufacturing*, Vol. 36, p. 101415, dec 2020.

100. Chadha, A., M. I. Ul Haq, A. Raina, R. R. Singh, N. B. Penumarti, and M. S. Bishnoi, "Effect of fused deposition modelling process parameters on mechanical properties of 3d printed parts," *World Journal of Engineering*, Vol. 16, p. 550–559, July 2019.

101. Bayas, E., P. Kumar, and K. Deshmukh, "A comprehensive review: Process parameters impact on tensile strength of 3d printed pla parts," *International Journal of Advanced Research in Science, Communication and Technology*, 2023.

102. Castillo, M., R. Monroy, and R. Ahmad, "Design of experiments to compare the mechanical properties of polylactic acid using material extrusion three-dimensional-printing thermal parameters based on a cyber–physical production system," *Sensors*, Vol. 23, p. 9833, dec 2023.

103. Kubota, M., K. Hayakawa, and A. Todoroki, "Effect of build-up orientations and process parameters on the tensile strength of 3d printed short carbon fiber/pa-6 composites," *Advanced Composite Materials*, Vol. 31, p. 119–136, June 2021.